**TP 12123E**

# Small-Scale BLEVE Tests with Refrigerant-22

*Prepared for*

Transportation Development Centre
Safety and Security
Transport Canada

*by*

D. L. Frost, R. Barbone, and J. Nerenberg
Department of Mechanical Engineering,
McGill University,
Montreal, Quebec,
H3A 2K6

December 1995

## DISCLAIMER

The contents of this report reflect the views of the authors and not necessarily the official views of the Transportation Development Centre.

The Transportation Development Centre does not endorse products or manufacturers. Trade or manufacturers' names appear in this report only because they are essential to its objectives.

## LANGUAGE NOTICE

Un sommaire en français de ce rapport est inclus avant la table des matières.

Transport Canada / Transports Canada

# PUBLICATION DATA FORM

| 1. Transport Canada Publication No. | 2. Project No. | 3. Recipient's Catalogue No. |
|---|---|---|
| TP 12123E | 8046 | |

| 4. Title and Subtitle | 5. Publication Date |
|---|---|
| Small-Scale BLEVE Tests with Refrigerant-22 | December 1995 |
| | 6. Performing Organization Document No. |

| 7. Author(s) | 8. Transport Canada File No. |
|---|---|
| D. Frost, R. Barbone, J. Nerenberg | 1465-302-11-4 |

| 9. Performing Organization Name and Address | 10. PWGSC File No. |
|---|---|
| Dept. of Mechanical Engineering<br>McGill University<br>817 Sherbrooke St. W.<br>Montreal, Quebec<br>H3A 2K6 | XSD92-00100-(673) |
| | 11. PWGSC or Transport Canada Contract No.<br>T8200-2-2520/01-XSD |

| 12. Sponsoring Agency Name and Address | 13. Type of Publication and Period Covered |
|---|---|
| Transportation Development Centre (TDC)<br>800 René Lévesque Blvd. West<br>6th Floor<br>Montreal, Quebec<br>H3B 1X9 | Final |
| | 14. Project Officer<br>W.S.C. McLaren |

15. Supplementary Notes (Funding programs, titles of related publications, etc.)

Cosponsored by the Dangerous Goods Directorate

16. Abstract

The rapid boiling that occurs when a pressure-liquefied gas (Refirgerant 22) is suddenly vented to the atmosphere was investigated at small scale in three geometrically dissimilar vessels (a rectangular steel vessel and cylindrical and spherical glass vessels). Fast-response piezoelectric pressure transducers and high-speed photography were used to monitor the pressure history within the vessel and record the evolution of the boiling process. The influence of the vent area, initial liquid fill volume and initial pressure on the rate and amount of repressurization was studied and the results are presented within this report.

Measurements clearly show that the degree of repressurization is proportional to the pressure drop and the non-dimensional degree of superheat attained by the liquid following depressurization. Although photographic evidence illustrates that heterogeneous boiling dominates in the current vessel, the results suggest that there is an initial pressure level that represents the "most dangerous" situation in terms of the boiling response of the liquid subjected to a pressure drop. This behaviour appears to depend on the thermodynamics of the liquid and is not sensitive to the detailed geometry of the vessel or the liquid fill volume. From the point of view of prevention of a violent BLEVE, the current results also suggest that situations leading to large rates and degrees of depressurization, corresponding to higher levels of superheat attained by the liquid, should be avoided.

| 17. Key Words | 18. Distribution Statement |
|---|---|
| BLEVE, small scale tests, explosive boiling, rapid venting, repressurization | Limited number of copies available from the Transportation Development Centre |

| 19. Security Classification (of this publication) | 20. Security Classification (of this page) | 21. Declassification (date) | 22. No. of Pages | 23. Price |
|---|---|---|---|---|
| Unclassified | Unclassified | — | xiv, 34 | Shipping/ Handling |

Transports Canada Transport Canada

# FORMULE DE DONNÉES POUR PUBLICATION

| 1. N° de la publication de Transports Canada | 2. N° de l'étude | 3. N° de catalogue du destinataire |
|---|---|---|
| TP 12123E | 8046 | |

| 4. Titre et sous-titre | 5. Date de la publication |
|---|---|
| Small-Scale BLEVE Tests with Refrigerant-22 | Décembre 1995 |
| | 6. N° de document de l'organisme exécutant |

| 7. Auteur(s) | 8. N° de dossier - Transports Canada |
|---|---|
| D. Frost, R. Barbone, J. Nerenberg | 1465-302-11-4 |

| 9. Nom et adresse de l'organisme exécutant | 10. N° de dossier - TPSGC |
|---|---|
| Dept. of Mechanical Engineering<br>McGill University<br>817 Sherbrooke St. W.<br>Montreal, Quebec<br>H3A 2K6 | XSD92-00100-(673) |
| | 11. N° de contrat - TPSGC ou Transports Canada |
| | T8200-2-2520/01-XSD |

| 12. Nom et adresse de l'organisme parrain | 13. Genre de publication et période visée |
|---|---|
| Centre de développement des transports (CDT)<br>800, boul. René-Lévesque Ouest<br>6e étage<br>Montréal (Québec)<br>H3B 1X9 | Final |
| | 14. Agent de projet |
| | W.S.C. McLaren |

15. Remarques additionnelles (programmes de financement, titres de publications connexes, etc.)

Recherche coparrainée par la Direction Transport de marchandises dangereuses.

16. Résumé


Le phénomène de vaporisation et de montée en pression rapides qui se produit lorsqu'un gaz liquéfié sous pression (en l'occurrence un gaz frigorigène R-22) est soumis à une détente brutale a été approfondi par des expérimentations utilisant des récipients de faible capacité, différents tant par leur forme géométrique que par le matériau dont ils sont faits : récipient rectangulaire en acier, cylindrique et spérique en verre. Les réactions et l'évolution des pressions ont été enregistrées à l'aide de capteurs de pression piézoélectriques et de caméras ultra-rapides. L'influence de divers paramètres tels que la dimension de la rupture, le niveau de remplissage et la pression initiale sur le régime de remontée en pression a été observée et les observations consignées dans le rapport produit.

Il a été observé que la remontée en pression du contenu est proportionnelle à la chute de pression ainsi qu'au degré de surchauffe (grandeur adimensionnelle) résultant de cette chute. Bien que les images photographiques montrent que l'ébullition qui s'amorce a un caractère essentiellement hétérogène, il a été observé qu'il existe une pression initiale donnant lieu à une réaction caractérisée comme la «plus dangereuse» en termes d'ébullition soudaine du contenu consécutive à une détente brutale. Il semble que cette réaction soit liée davantage à l'état thermodynamique du contenu qu'à la géométrie du récipient ou qu'au niveau de remplissage. Pour ce qui est de la prévention des explosions de rupture, les résultats semblent indiquer qu'il faudra éviter les conditions pouvant donner lieu à des détentes fortes et brutales s'accompagnant d'une forte surchauffe du contenu.


| 17. Mots clés | 18. Diffusion |
|---|---|
| Explosion de rupture, essais à petite échelle, ébullition donnant lieu à une explosion, explosion à la pression atmosphérique, formation de pression | Le Centre de développement des transports dispose d'un nombre limité d'exemplaires. |

| 19. Classification de sécurité (de cette publication) | 20. Classification de sécurité (de cette page) | 21. Déclassification (date) | 22. Nombre de pages | 23. Prix |
|---|---|---|---|---|
| Non classifiée | Non classifiée | — | xiv, 34 | Port et manutention |

## ACKNOWLEDGEMENTS

The authors would like to thank Dr. Aris Makris, Ernesto Piñal, Jean-François Lebel and Christine Desmarais for assistance in carrying out the experiments. The lead author would also like to thank the other university researchers working with Transport Canada on the BLEVE phenomenon, particularly Prof. Mike Birk of Queen's University, and Profs. Frank Stewart and Jim Venart of the University of New Brunswick, for their insight and suggestions regarding the small-scale work. Financial support for this work was provided by Transport Canada under DSS Contract T8200-2-2520/01-XSD.

# EXECUTIVE SUMMARY

When a pressure-liquefied gas contained within a tank is suddenly vented the ensuing rapid vapor generation and pressure buildup may lead to the catastrophic failure of the containment vessel. Such an event is often referred to as a BLEVE, or boiling-liquid-expanding-vapor-explosion to acknowledge the role of the rapid boiling of the liquid in the explosion process. Hazards associated with BLEVEs include the initial blast wave, radiation from a fireball if the tank contents are flammable and flying projectiles. Accidental BLEVEs have caused extensive damage in the past, both in stationary storage facilities containing pressure-liquefied gases as well as during the transportation of hazardous pressurized liquids.

One accident scenario for a BLEVE involves the derailment of a tank car carrying a flammable pressure-liquefied gas such as propane. Partial release of the contents of one tank may lead to a fire which impinges on adjacent tank cars. The fire impingement increases the temperature of the tank wall which induces boiling of the liquid within the tank. The liquid temperature and corresponding saturation pressure both increase. The increasing tank temperature also reduces the strength of the tank wall material and at some point the structural integrity of the tank will fail. At this point several different events may occur. Complete failure of tank walls may occur if the pressure inside the tank is sufficiently high whereas a benign venting of the tank contents may occur if the initial pressure is lower and a finite sized vent hole is formed. An intermediate case occurs if the liquid within the tank is partially vented by the formation of a crack. In this case, the subsequent rapid boiling of the liquid may lead to substantial repressurization within the vessel which may then initiate complete failure of the vessel. The degree of repressurization will depend on the competition between the rates of venting and vapor generation which in turn will depend on the vent area as well as the thermodynamic conditions of the liquid and properties of the vessel surface.

The present study was carried out to determine the conditions that lead to the greatest degree of repressurization following the sudden depressurization of a pressure-liquefied gas contained within a vessel. The parameters that were varied in the present study include the initial thermodynamic state of the liquid, the fill volume, vent area, vessel wall material and geometry and the presence of nucleation sites within the liquid. The experiments were carried out at small scale (vessel volumes < 1 l) in steel and glass-walled vessels. The test liquid used was Refrigerant-22, which has very similar thermodynamic properties to propane yet is not flammable. Depressurization of the test liquid was obtained by rupturing a metal diaphragm with a pneumatically-actuated plunger. The pressure history inside the vessel was monitored with a fast-response piezoelectric pressure transducer and the boiling process inside the vessel was visualized with high-speed photography.

The most important finding of the present study is that the degree of repressurization reaches a maximum value as the initial pressure of the liquid is increased. The maximum repressurization occurs near an initial pressure that corresponds to the state at which the maximum degree of superheat may be obtained, if the pressure were to drop to atmospheric pressure. A similar behavior was obtained for all three test section geometries tested (rectangular, cylindrical and spherical). The repressurization time is typically more than an order of magnitude larger than the time for the initial pressure drop. The degree of repressurization is proportional to the pressure

drop and the non-dimensional degree of superheat attained by the liquid following the drop in pressure. For high initial pressures, photographic evidence shows that the boiling process is dominated by heterogeneous boiling from the walls of the liquid. For the glass-walled vessels, below a critical initial pressure (of about 1 MPa), boiling from the vessel walls is suppressed, and boiling is initiated at the free surface and propagates into the superheated liquid in a wave-like fashion. Downstream of this evaporation wave, a high-speed two-phase flow is generated. Placing a quantity of steel wool inside the test section promotes nucleation within the bulk of the liquid. In this case, the degree of depressurization is reduced although due to the increased number of nucleation sites within the liquid, the degree of repressurization is generally increased.

The present results indicate that when a pressure-liquefied gas is suddenly depressurized, there exists an initial pressure level which represents the "most dangerous" situation in terms of the boiling response of the liquid. Since this behavior appears to depend more on the thermodynamics of the liquid than on the detailed geometry of the vessel, this result may also apply to larger scale systems. From the point of view of prevention of a violent BLEVE, the current results suggest that situations leading to large rates and degrees of depressurization (e.g., large vent areas and liquid fill volumes, smooth vessel wall surfaces), corresponding to higher levels of superheat attained by the liquid, should be avoided. Enhancing the number of nucleation sites within the bulk of the liquid may reduce the rate and amount of the pressure drop, but may actually lead to an increase in the repressurization within the vessel.

# SOMMAIRE

Lorsqu'un gaz liquéfié sous pression dans un réservoir est soumis à une détente brutale, il se produit une vaporisation et une montée en pression rapides qui peuvent faire éclater le réservoir dans ce qui est appelé une explosion de rupture ou BLEVE. Résultat de l'ébullition soudaine du liquide sous pression et de la dilatation des vapeurs qu'il dégage, cette explosion entraîne de graves conséquences. D'abord une conflagration, suivie d'un rayonnement thermique émanant de la boule de feu qui se forme si le liquide sous pression est inflammable et enfin la projection de fragments. Dans le passé, on a eu à déplorer plusieurs explosions de rupture aux conséquences catastrophiques, tant dans des installations où des gaz liquéfiés sous pression étaient stockés que durant le transport de matières inflammables sous pression.

Les circonstances entourant une explosion de rupture sont généralement les suivantes : un wagon-citerne transportant un gaz liquéfié sous pression inflammable tel que le propane déraille, laissant échapper une partie de sa cargaison. Si celle-ci vient à s'enflammer, les flames risquent alors de se propager vers les wagons adjacents dont les parois s'échaufferont rapidement, communiquant leur chaleur au contenu qui entre alors en ébullition. La température du gaz liquéfié augmentera ainsi que la pression de saturation correspondante. Simultanément la chaleur intense de l'incendie affaiblira la résistance des parois jusqu'à provoquer leur ruine en un point donné. À ce moment, plusieurs scénarios peuvent se produire : ruine totale des parois si la pression interne est suffisante; déversement sans danger du contenu si la pression initiale est faible et si l'ouverture est de dimension stable; ou, scénario intermédiaire, formation d'une fissure au travers de laquelle le gaz liquéfié se met à s'échapper. Dans ce dernier cas, la détente brutale qui se produit provoquera aussitôt l'ébullition du liquide suivie d'une remontée brutale de la pression qui serait l'amorce de la ruine totale des parois. Ce régime de remontée en pression dépendra de l'écart entre la vitesse à laquelle le liquide se vaporise et celle à laquelle il est évacué, cet écart dépendant à son tour de la dimension de la rupture, de l'état thermodynamique du contenu et de l'état de la surface interne des parois.

La présente recherche a cherché à determiner les paramètres qui maximisent la remontée en pression du contenu qui se produit à la suite d'une détente brutale à l'intérieur du wagon. La paramétrisation a porté sur les conditions thermodynamiques initiales du contenu, le niveau de remplissage, la dimension de la rupture, la nature du matériau dont est construit le contenant, la géométrie de celui-ci et le degré de nucléation du contenu. Les essais ont été faits à petite échelle, sur des récipients de capacité inférieure à 1 litre, en acier et en verre, remplis de R 22, gaz frigorigène dont les propriétés thermodynamiques sont très proches de celles du propane mais qui a l'avantage d'être ininflammable. La mise en contact brutale avec la pression ambiante a été réalisée par la perforation d'une membrane métallique à l'aide d'un poinçon pneumatique. Les réactions et l'évolution des pressions ont été enregistrées à l'aide de capteurs de pression piézoélectriques et de caméras ultra-rapides.

L'observation la plus intéressante qui a été faite est que la pression qui se recrée à l'intérieur du récipient atteint un plafond qui augmente à mesure qu'augmente la pression initiale, et que ce plafond est atteint lorsque celle-ci est proche de la pression initiale correspondant au degré maximum de surchauffe qu'il est possible d'obtenir lorsque la pression saturée du liquide est brutalement ramenée à la pression ambiante. Les mêmes réactions ont été observées pour les

trois formes géométriques mises en oeuvre : rectangulaire, cylindrique et sphérique. Il a été observé que la remontée en pression est généralement plus rapide que la chute de pression initiale par plus qu'un ordre de grandeur, et qu'elle est proportionnelle à celle-ci ainsi qu'au degré de surchauffe (grandeur adimensionnelle) résultant de cette chute. Les images photographiques prises montrent qu'aux pressions initiales élevées, l'ébullition qui s'amorce aux parois montre un caractère essentiellement hétérogène. Dans le cas des récipients en verre, on constate l'absence d'ébullition aux parois jusqu'à une pression initiale inférieure à environ 1 Mpa, l'ébullition s'amorçant plutôt à la surface libre et se propageant sous forme d'onde au contenu en surchauffe. À l'aval de cette onde d'évaporation, on observe un écoulement diphasique rapide. Une quantité de laine d'acier placée dans le récipient favorise la nucléation à l'intérieur même du contenu. On constate un ralentissement dans la vitesse à laquelle la pression décroît bien que le régime de remontée en pression ait tendance à augmenter en raison du nombre accru de points de nucléation créés à l'intérieur du liquide.

Lorsque le contenu subit une détente brutale, un état de pression initiale est créé donnant lieu à une réaction caractérisée comme la «plus dangereuse» en termes d'ébullition soudaine du contenu.

Étant donné que cette réaction semble liée plus à l'état thermodynamique du contenu qu'à la géométrie du récipient, on s'autorise à dire qu'elle se produira également dans les récipients de plus grande capacité. Pour ce qui est de la prévention des explosions de rupture, les résultats semblent indiquer qu'il faudra éviter les conditions pouvant donner lieu à des détentes fortes et brutales (orifices d'évacuation de fortes dimensions, niveaux de remplissage élevés, réservoirs à parois intérieures lisses) s'accompagnant d'une forte surchauffe du contenu. Le fait d'augmenter les points de nucléation à l'intérieur du contenu pourrait atténuer la force et la brutalité des détentes, au risque toutefois de mener à un régime de remontée en pression encore plus prononcé.

# CONTENTS


1. INTRODUCTION ..... 1
   1.1 Theoretical Considerations ..... 2
   1.2 Objectives ..... 4

2. EXPERIMENTAL APPARATUS ..... 5
   2.1 General Description of Apparatus ..... 5
   2.2 Rectangular Steel Pressure Vessel ..... 7
   2.3 Cylindrical Glass Vessel ..... 8
   2.4 Spherical Glass Test Vessel ..... 11
   2.5 Diagnostic Systems ..... 12
   2.6 Test Fluid ..... 13

3. RESULTS AND DISCUSSION ..... 15
   3.1 General Features of Pressure History ..... 15
   3.2 Parametric Investigation with Rectangular Steel Vessel ..... 17
      3.2.1 Visualization of Boiling in Rectangular Steel Vessel ..... 21
   3.3 Parametric Investigation with Cylindrical Glass Vessel ..... 22
      3.3.1 Visualization of Boiling in Cylindrical Glass Vessel ..... 22
   3.4 Parametric Investigation with Spherical Glass Vessel ..... 29
      3.4.1 Visualization of Boiling in Spherical Glass Vessel ..... 31

4. CONCLUSIONS AND RECOMMENDATIONS ..... 32

REFERENCES ..... 33

## LIST OF FIGURES


Fig. 1.1 p-T diagram for R-22 illustrating thermodynamic path during sudden depressurization. The spinodal curve is the locus of superheat limit points. ..... 3

Fig. 2.1 Overview of rapid depressurization facility. ..... 5

Fig. 2.2 Plunger system used to initiate depressurization. ..... 6

Fig. 2.3 Schematic of steel vessel with rectangular test section. ..... 7

Fig. 2.4 Schematic diagram of cylindrical glass test section within outer pressure vessel. ..... 9

Fig. 2.5 Schematic diagram of interior of pressure vessel containing cylindrical glass test section ..... 10

Fig. 2.6 Schematic diagram of collar that holds and seals 50 ml spherical test section. ..... 11

Fig. 2.7 Schematic diagram of high-speed photography setup. ..... 12

Fig. 2.8 Comparison of liquid-vapor saturation curves for Refrigerant-22 and propane. ..... 14

Fig. 3.1 Comparison of characteristic pressure history for venting of R-22 and pressurized water ..... 15

Fig. 3.2 Pressure history recorded for horizontal test section illustrating pressure spikes generated by impact of liquid droplets with pressure transducer face. ..... 16

Fig. 3.3 Effect of orifice area on pressure history for 90% liquid fill. ..... 17

Fig. 3.4 Effect of orifice area on degree of depressurization and repressurization. ..... 18

Fig. 3.5 Effect of initial liquid volume on pressure history. Initial pressure is 3.15 MPa. ..... 18

Fig. 3.6 Effect of liquid fill volume on the degree of depressurization and repressurization. ..... 19

Fig. 3.7 Relationship between pressure rise and pressure drop for trials with steel vessel. ..... 19

Fig. 3.8 Degree of repressurization as a function of initial pressure within steel vessel. The curve represents a second order polynomial fit through the 65% fill data.....20

Fig. 3.9 Locus of thermodynamic end states following pressure drop showing the degree of superheat attained for the steel test vessel. .....21

Fig. 3.10 Sequence of high-speed photographs showing heterogeneous boiling of R-22 from the walls in the 260 ml steel vessel ($P_i$ = 1.03 MPa). .....22

Fig. 3.11 Sequence of high-speed photographs showing heterogeneous boiling of R-22 from the walls of steel vessel with an initial pressure of 1.43 MPa.....23

Fig. 3.12 Normalized pressure rise as a function of normalized pressure drop for the 75 ml cylindrical glass vessel. .....24

Fig. 3.13 Pressure drop and rise as a function of the initial pressure in the 75 ml cylindrical glass vessel. .....24

Fig. 3.14 Breakup of free surface of liquid R-22 contained within a glass tube following depressurization ($P_i$ = 1.20 MPa). .....25

Fig. 3.15 Sequence of high-speed photographs showing the propagation of an evaporation wave into superheated R-22 in a glass tube ($P_i$ = 1.03 MPa). .....26

Fig. 3.16 Contours (shown as a mirror image) of the boiling front shown in Fig. 3.15.....27

Fig. 3.17 Variation of displacement and velocity of evaporation wavefront estimated from Fig. 3.16. .....27

Fig. 3.18 Sequence of high-speed photographs illustrating the heterogeneous nucleation on the wall of the glass tube for an initial pressure of 2.24 MPa.....28

Fig. 3.19 Normalized pressure rise as a function of normalized pressure drop for 150 ml spherical glass vessel with 90% liquid fill volume and an orifice diameter of 2.54 cm. .....29

Fig. 3.20 Repressurization as a function of initial vessel pressure for the spherical glass vessel with 90% liquid fill volume. .....30

Fig. 3.21 Comparison of the repressurization as a function of initial vessel pressure with and without the presence of a ball of steel wool within the bulk of liquid. ..... 30

Fig. 3.22 Sequence of high-speed photographs showing the propagation of an evaporation wave within a 50 ml glass sphere. The initial liquid free surface is located at the junction between the sphere and the neck. ..... 31

# 1. INTRODUCTION

If a liquid is suddenly superheated, the stored thermal energy can be released explosively during the subsequent rapid phase transition. This rapid boiling process can occur, for example, when a volatile liquid stored under pressure is suddenly depressurized. This phenomenon, when associated with the catastrophic failure of railway tank cars and storage vessels containing pressure-liquefied gases, is often referred to as a BLEVE, or Boiling Liquid Expanding Vapor Explosion (Reid, 1979). If the vessel contains a combustible liquid such as propane, the dispersion of the tank contents in the form of a two-phase jet can generate a blast wave and a destructive fireball if an ignition source is present. Such accidents have caused extensive damage in the past (e.g., see Wormuth, 1985) and provide the motivation for the fundamental study of the rapid boiling of a depressurized volatile liquid.

If a pressurized volatile liquid contained within a vessel is partially vented (by the formation of a crack or the action of a pressure relief valve), rapid boiling of the liquid may lead to substantial repressurization within the vessel which may then initiate the complete failure of the vessel. The degree of repressurization will depend on the competition between the rates of venting and vapor generation. The dependence of the rate and amount of repressurization on the vessel geometry and the initial thermodynamic state of the liquid has not been studied extensively in the past.

Past experimental work on explosive boiling due to sudden depressurization has ranged from prototypical scale tests involving railway and automotive tanks containing pressure-liquefied gases to small-scale studies investigating the fundamental dynamics of the boiling of a depressurized liquid. On an intermediate scale, Birk et al. (1991, 1994) have studied the explosion of 400 L automotive propane tanks subjected to a pool fire. They observed several different types of failure sequences, depending on the strength of the tank and the energy contained within the tank. For weak-walled tanks, catastrophic failure of the tank was attributed to the energy associated with the pressurized vapor. Long-duration failures occurred in which a crack initially formed followed by catastrophic vessel failure after a delay of up to 3 s. In this case, they attributed the tank failure to the boiling response of the liquid. They found by plotting the results on a "BLEVE map" using the tank burst pressure and the liquid temperature scaled with the fill level, that the BLEVE and non-BLEVE results were clearly separated. For strong-walled tanks they observed that BLEVEs occurred only above a threshold liquid temperature. Important conclusions from their results with practical implications were that the pressure relief valve set pressures and the tank wall thickness had a significant effect on whether the tank would BLEVE or not. However, the difficulty in obtaining reliable rapid pressure measurements within the tank prevented them from obtaining detailed dynamic information on the behavior of the liquid inside the tank.

Friedel and Purps (1986) and Hervieu (1992) have studied the blowdown of refrigerant and propane tanks, respectively, with emphasis on the two-phase venting behavior. The pressure behavior observed by Friedel and Purps (1986) during tank venting is qualitatively similar to the present smaller scale tests. However, the tanks were depressurized using fast-opening valves which resulted in rates of depressurization typically several orders of magnitude smaller than those in the present study.

In a study similar to the present investigation, Hanaoka et al. (1990) carried out experiments in which 300–600 ml of refrigerant (R-113 or R-11) contained inside a glass tube (5 cm id) was depressurized by opening a solenoid valve. The pressure history they recorded within the vessel was similar to that of the present investigation although, due to the opening time of the valve, the depressurization time was typically an order of magnitude larger than the present study. They defined a nondimensional "flashing violence factor" which was the product of the amount of repressurization and the amount of the liquid that was expelled from the vessel. They found that the violence factor was increased when a metal rod was placed inside the vessel, due to an enhanced rate of nucleation.

At small scale, detailed fundamental photographic studies of the boiling of depressurized liquids have been carried out by Hill and Sturtevant (1989) and Chaves (1985). They observed the details of the two-phase evaporation wave that propagated into a superheated liquid within a vertical glass tube. In both cases the venting rate was large and no repressurization was observed within the tube.

## 1.1 Theoretical Considerations

To facilitate the understanding of the rapid depressurization of tanks containing pressure-liquefied gases (PLG) and the subsequent boiling, it is instructive to consider the thermodynamic path taken by the liquid following diaphragm rupture. A sudden drop of pressure from an initial state where the liquid and vapor phases are in equilibrium will result in a reduction of the pressure below the saturation pressure at the initial temperature. Such a sudden drop in pressure will superheat the liquid. The degree of superheat is defined by the degree by which the state of the liquid has surpassed the saturation state. The superheat is normally expressed as the difference between the final temperature and the saturation temperature at the pressure of the depressurized state, i.e., $\Delta T = T_f - T_{sat}(p_f)$. Figure 1.1 shows the depressurization process on a pressure-temperature curve, as well as the saturation and spinodal curves. The thermodynamic state of the liquid follows an isentropic expansion from $p_i$, initially on the saturation curve, to a final pressure of $p_f$. For the initial temperature range of interest the isentropic depressurization is well approximated by an isothermal expansion on the $p$-$T$ diagram, so the final temperature $T_f \approx T_i$. The decrease in system pressure below its saturation pressure at the initial temperature, will cause the liquid-vapor equilibrium to be disrupted and thus induce boiling to regenerate the pressure and re-establish equilibrium.

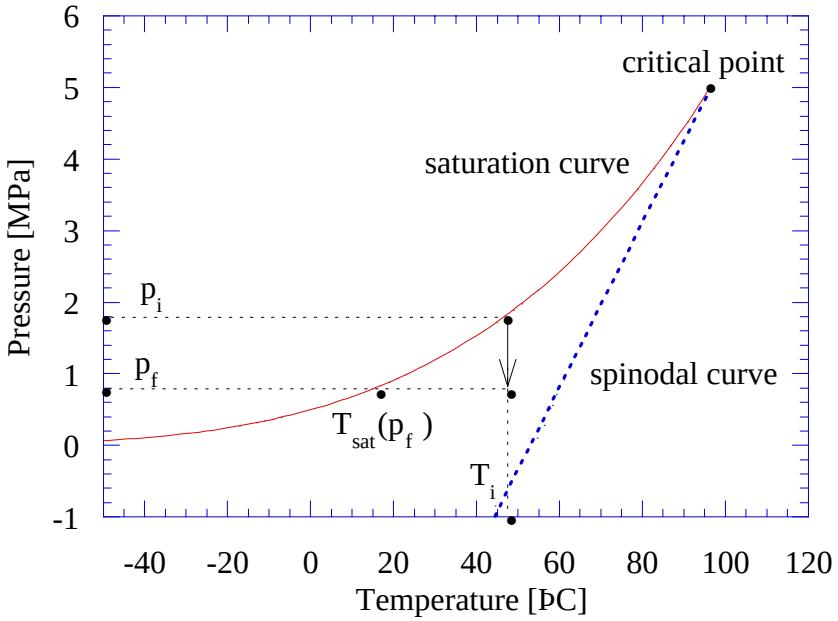


Fig. 1.1 p-T diagram for R-22 illustrating thermodynamic path during sudden depressurization. The spinodal curve is the locus of superheat limit points.

The amount of superheat attainable for a given substance is finite and limited by thermodynamic and physical constraints. The spinodal curve and the saturation curve form the boundary for the metastable region. In the metastable region a liquid can be superheated and a vapor supersaturated without a phase change, even though the states lie inside the two phase dome. The spinodal curve is therefore a thermodynamic limit beyond which a liquid cannot remain in the liquid state and as a consequence nucleation sites grow rapidly within the bulk of the liquid when the superheat limit is attained (this is referred to as homogeneous nucleation). If a liquid is brought uniformly to the superheat limit, a violent vapor explosion will occur. The dynamics of the boiling of a highly superheated liquid has been extensively studied in the past and for a general review of superheated liquids, the reader is referred to the book by Skripov (1974) or the review by Avedisian (1986).

If bubbles or other nucleation sites are present within the liquid prior to depressurization, the threshold for boiling to begin is lowered, limiting the amount of depressurization that can be attained. In the present experimental investigation the rapid depressurization does not permit the fluid state to reach the spinodal due to physical constraints. Foreign bodies and container surfaces provide nuclei to act as centers for vapor formation (this process is referred to as heterogeneous nucleation). Examples of pre-existing nuclei are dissolved gases and vapor trapped in microscopic cracks and scratches on the container surfaces. The presence of pre-existing nuclei has the effect of reducing the degree of superheat attained below the maximum

value predicted by the thermodynamic superheat limit and is illustrated in Fig. 1.1. Although heterogeneous boiling is expected to be dominant in most rapid depressurization scenarios involving a volatile liquid stored in a vessel, the subsequent repressurization within the vessel may nevertheless pose a serious threat to the container integrity.

The rapid depressurization of hot saturated water in a pipe has been studied extensively due to its relevance to nuclear reactor safety although in this case little repressurization is observed (e.g., Bartak, 1990). For this case, Alamgir and Lienhard (1981) have developed a semi-empirical model to predict the pressure undershoot. Their model is based on the assumption that if the rate of depressurization is large enough and the size of any physical heterogeneity present is small enough, then nucleation is initiated stochastically and is governed by homogeneous nucleation theory. To account for nucleation at the wall, they introduce a heterogeneous correction factor (which is determined by fitting to experimental data) to the Gibbs number, which is a measure of the potential barrier to nucleation. Application of the correlation to the present experimental data is described in Barbone (1994).

## 1.2 Objectives

The objective of the present study is to investigate, by means of high-speed photography and fast-response pressure instrumentation, the dynamics of the boiling of a volatile liquid within a rigid walled vessel which is rapidly depressurized by bursting a foil diaphragm. In particular, we have concentrated on determining how the rate and amount of repressurization that occurs within the vessel following rapid venting depends on the initial and boundary conditions. Prior to diaphragm rupture, the liquid is in a saturation state. The small scale of the experiments permits a uniform temperature to be attained throughout the pressurized liquid and allows good control over the parameters that influence the pressure history within the vessel. Such parameters include the liquid fill volume, the vent area, the surface conditions of the vessel and the existence of nucleation sites within the bulk of the liquid. Refrigerant-22 (R-22) is used as the test liquid since it exhibits similar thermodynamic properties to propane, and yet is not flammable. The goal of this study is to determine the conditions that can lead to the maximum repressurization within a vessel, i.e., the worst case scenario from the point of view of the prevention of a violent BLEVE.

# 2. EXPERIMENTAL APPARATUS

## 2.1 General Description of Apparatus

An overview of the rapid depressurization facility used in the present study is shown in Fig. 2.1. The facility can accommodate test sections with several different geometries. A rectangular steel chamber (with Teflon coating) was used as well as cylindrical and spherical glass vessels. The glass vessels were placed inside a larger steel pressurized vessel to allow higher initial pressures to be reached and to contain the vessel in the event of the bursting of the glass vessel.

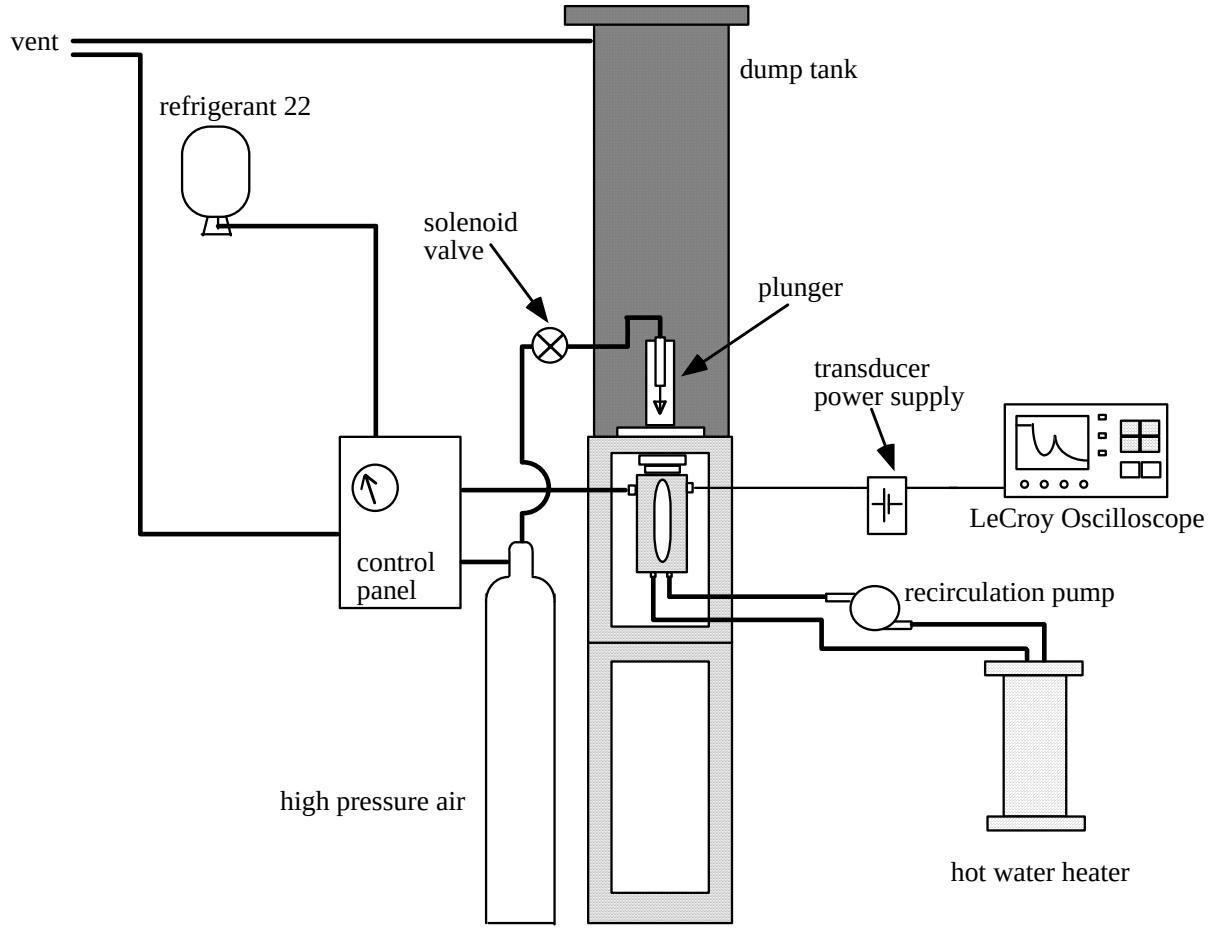


Fig. 2.1 Overview of rapid depressurization facility.

The depressurization apparatus includes a frame that holds the test section and a 0.13 $m^3$ steel dump tank placed above the test section, downstream of the foil diaphragm on the top of the test section. In all experiments the dump tank initially contains air at atmospheric pressure. To depressurize the test section, a pneumatic plunger with a spear tip is used to burst a foil diaphragm. All vessels used were sealed with a diaphragm with thickness varying from 25–100

μm depending on the initial pressure within the vessel. The plunger system, contained within the dump tank directly above the pressure vessel and shown schematically in Fig. 2.2, is attached to a high-pressure air cylinder with a solenoid valve. To initiate an experiment the air line is pressurized to 1 MPa, and the solenoid is opened.

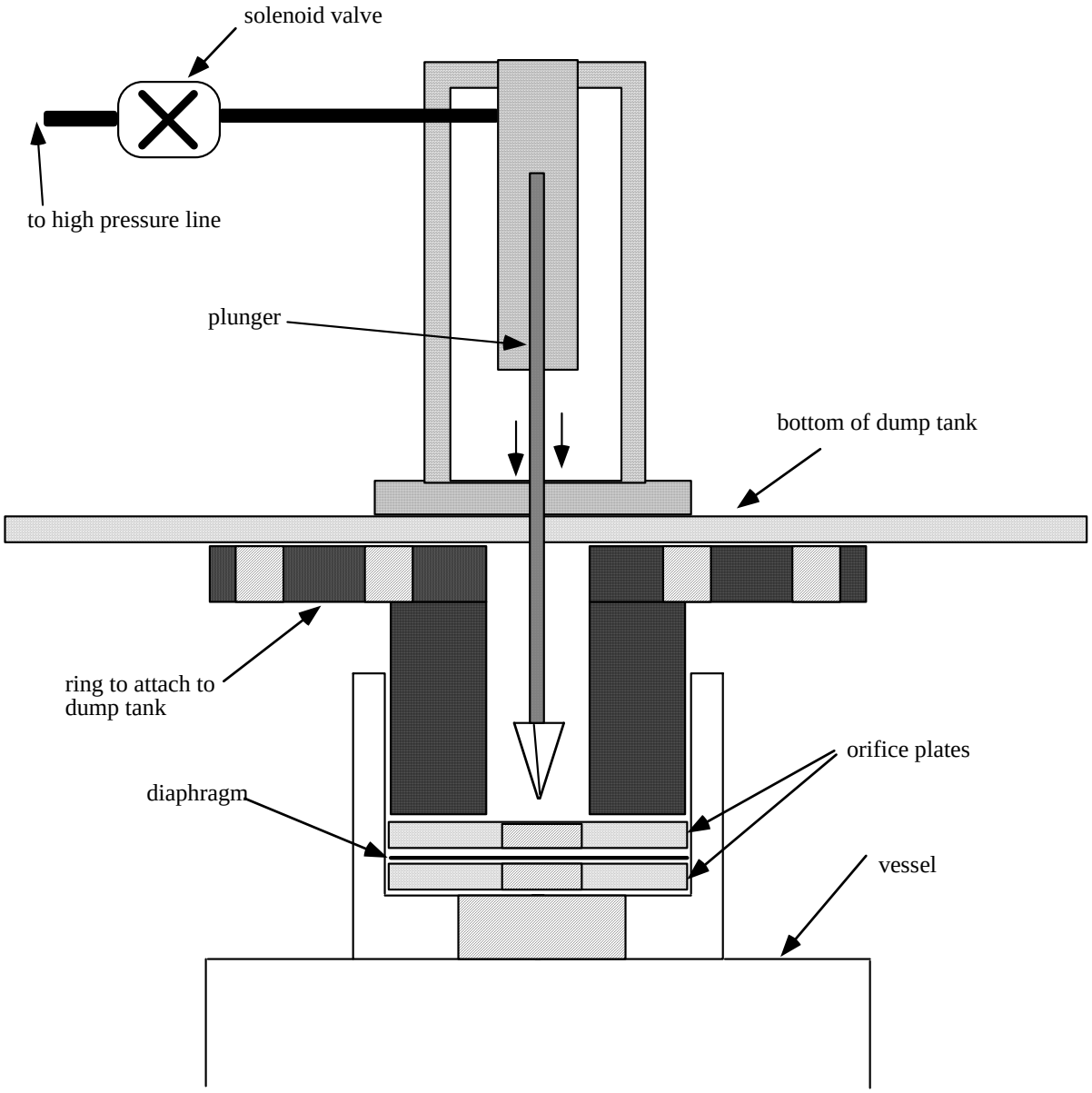


Fig. 2.2 Plunger system used to initiate depressurization.

To control the initial temperature of the refrigerant-22, hot water was pumped through heating tubes within the vessels. A hot water reservoir with a 1500 W heater was used to raise the temperature of the water, and a Little Giant Pump (Model 2-MD-HC) magnetic drive pump was used to circulate the water through the heating elements in the pressure vessels. Three different vessel were used as test sections and are described below in detail.

## 2.2 Rectangular Steel Pressure Vessel

The first vessel used was a Teflon-coated steel-walled vessel shown schematically in Fig. 2.3. This vessel simply consists of a 7.5 cm x 7.5 cm x 28 cm block of steel with a vertical slot milled out of its center where the test liquid is held during an experiment. The dimensions of this slot are approximately 2 cm wide x 19 cm high x 7.5 cm deep forming a test section with a volume of about 260 ml. The slot passes through the block of steel and is covered on each end by 2 cm thick glass windows for visualization. The vessel walls were Teflon-coated to eliminate rust and to minimize nucleation on the walls.

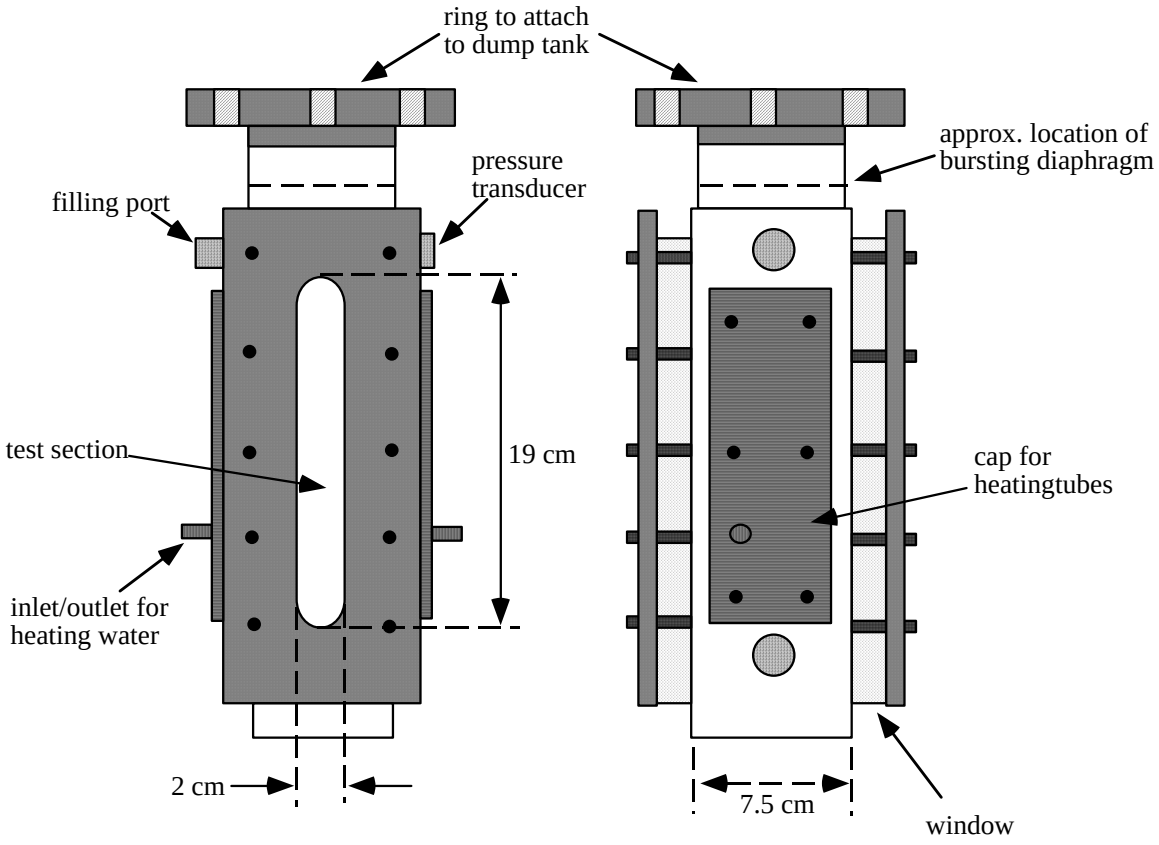


Fig. 2.3 Schematic of steel vessel with rectangular test section.

The top of the vessel holds the diaphragm, the orifice plates, and the ring to allow the vessel to be attached to the dump tank and the pneumatic plunger. The top of the vessel contains a 5 cm diameter hole into which two 0.5 cm thick round aluminum orifice discs are placed. The discs sandwich the foil diaphragm and contain a vent hole that was varied from 0.4 cm to 1.9 cm in diameter. The temperature of the refrigerant is controlled by circulating hot water through a labyrinth of slots milled on both sides of the pressure vessel. The vessel was filled with refrigerant through a port near the top of the test section. Another port near the top of the test section is used to house a piezoelectric pressure transducer that is used to monitor the pressure history inside the test section.

## 2.3 Cylindrical Glass Vessel

The second vessel used in this study consisted of a 75 ml cylindrical glass test tube (2.5 cm dia. x 15.2 cm long) shown in Fig. 2.4. The glass tube which contains the refrigerant is placed within an outer pressure vessel and held in place by Delrin moldings at the top and bottom of the vessel. The volume around the glass test tube was filled with glycerine to heat the refrigerant.

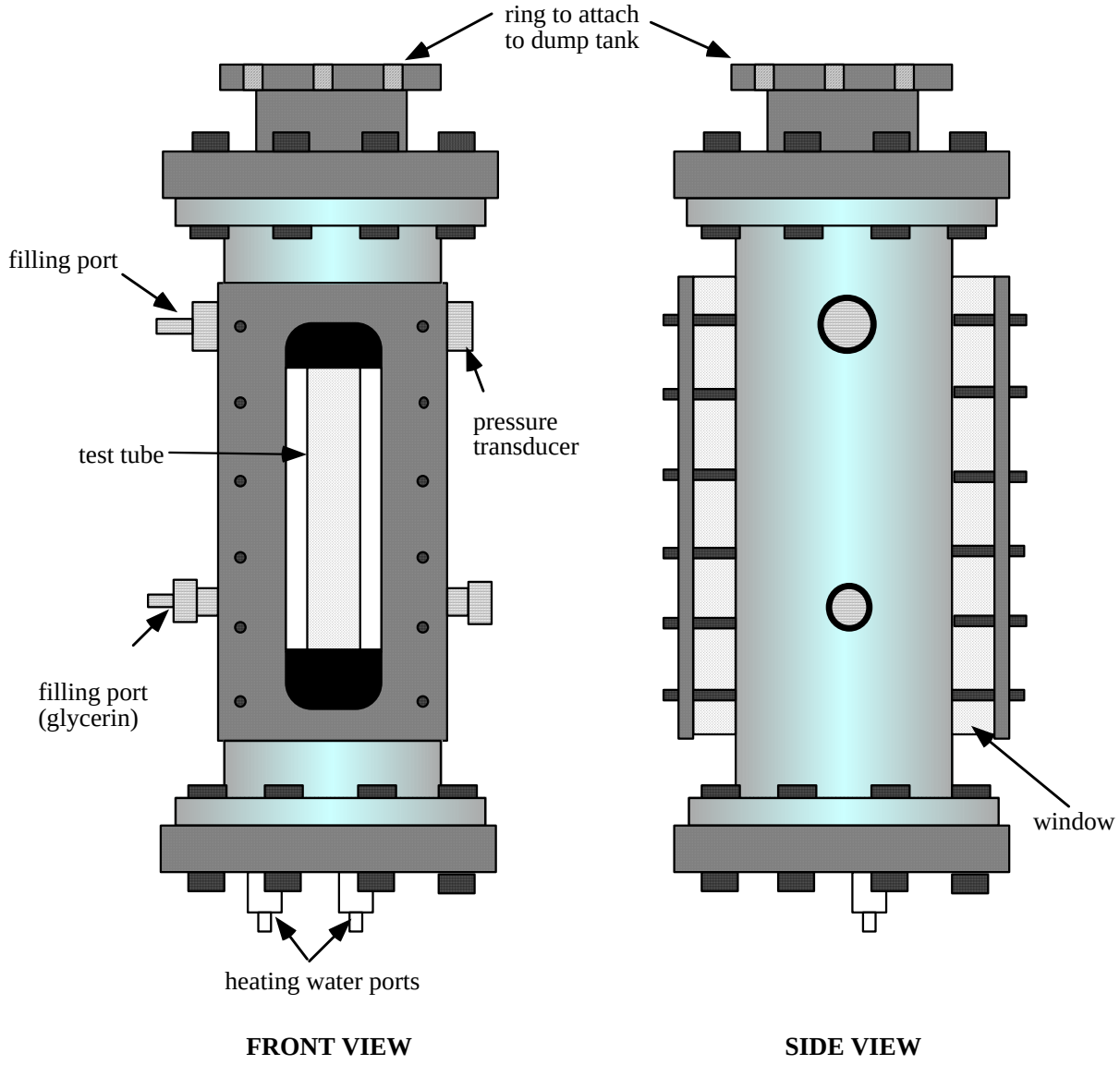


Fig. 2.4 Schematic diagram of cylindrical glass test section within outer pressure vessel.

This outer steel pressure vessel, although larger than the steel-walled vessel described earlier, is similar in that is has 2 cm thick glass windows to allow for visualization of the boiling process. The top of the vessel is also similar in that it houses the orifice plates, the diaphragm, and the ring to attach to the dump tank (see Fig. 2.5).

Heating and cooling the refrigerant in this vessel was accomplished by pumping water through a copper tube that runs along the length of the vessel through the space between the test tube and the vessel walls (see Fig. 2.5). To transfer the heat from these tubes to the refrigerant in the glass tube, glycerin was placed in the space between the test tube and the vessel walls. Glycerin was chosen because of it high viscosity to prevent sloshing during the depressurization process.

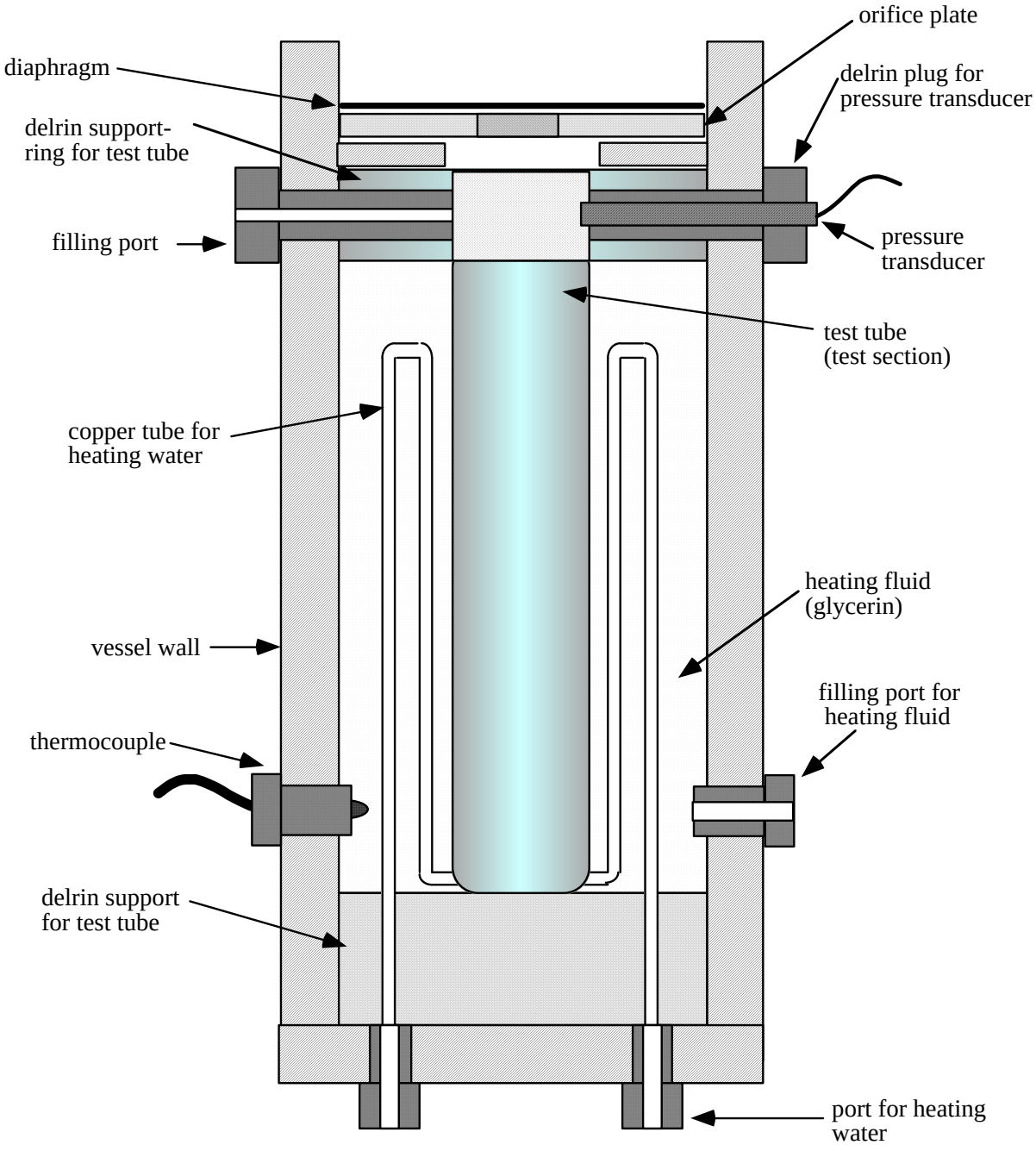


Fig. 2.5 Schematic diagram of interior of pressure vessel containing cylindrical glass test section.

For access to the test section this vessel has four ports; two near the vessel's top and two near its bottom. One top port was used to hold the plug containing the pressure transducer, while the other was used to fill the test tube and control the pressure of the vessel. Of the bottom ports, one was used to fill the glycerin into the test vessel around the test tube, while the other housed a thermocouple to monitor the temperature of the glycerin.

## 2.4 Spherical Glass Test Vessel

The third set of experiments was performed using a spherical Pyrex boiling flasks to contain the refrigerant. Initial trials were carried out with a 50 ml volume sphere and a systematic series of almost 200 trials was subsequently carried out with a 100 ml sphere (with a total volume of 150 ml including the neck). To integrate the glass spheres into the depressurization apparatus, an aluminum collar was designed to provide a pressure seal. The collar consists of a hollow cylinder, which splits in two. One end holds the neck of the boiling flask while the other holds the bursting diaphragm (see Fig. 2.6). As for the previous vessels the collar has ports: one is for filling the test fluid and the other holds the plug that houses the pressure transducer.

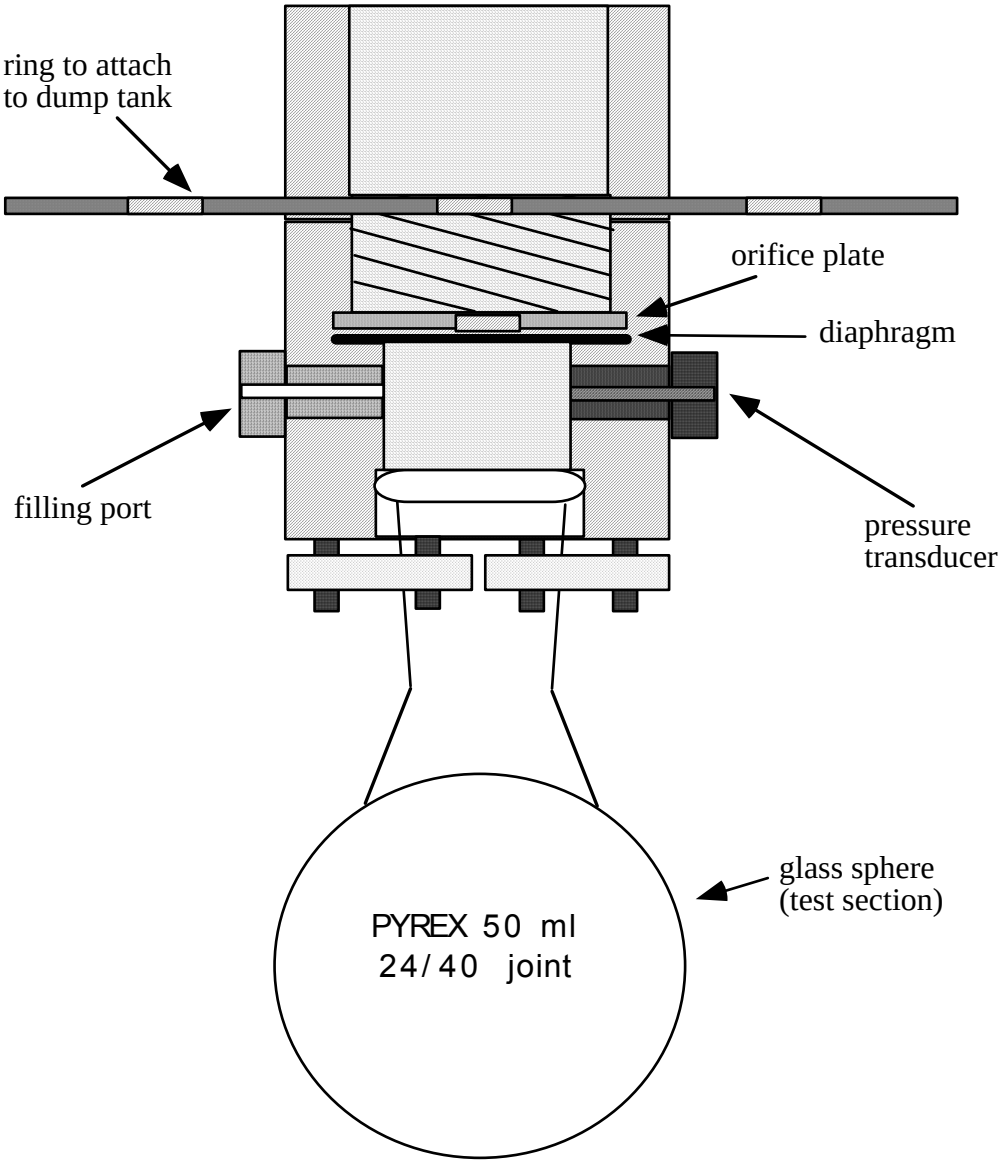


Fig. 2.6 Schematic diagram of collar that holds and seals 50 ml spherical test section.

The diaphragm is placed at the top end of the collar. The collar itself screws apart into two separate pieces. The diaphragm is placed in the lower end of the collar, with an orifice plate over it and the top end of the collar is screwed down to seal the diaphragm. To heat the refrigerant, a 20 cm diameter Plexiglas cylinder (1/2 cm wall thickness) was placed around the sphere and filled with water at the desired temperature. Since the burst pressure of the 100 ml spheres is about 1.5 MPa, the cylinder was pressurized so that a maximum pressure inside the sphere of about 2.5 MPa was attained.

Great care was taken to ensure that the inner surface of the glass sphere was as clean as possible prior to an experiment. This involved a routine of cleaning the sphere with alcohol between each trial. During a trial, the temperature of the heating water was increased very slowly. During this time boiling occurred at the surface of the vessel containing the refrigerant. To ensure that the temperature was uniform within the refrigerant prior to a trial, after the desired temperature was attained, the diaphragm was ruptured only after all the boiling had stopped and no convection was visible within the refrigerant (this could take several hours to occur at the higher temperatures).

## 2.5 Diagnostic Systems

To record the pressure/time history within the test section, a piezoelectric pressure transducer (Piezotronics PCB 113A24) was flush-mounted within a Delrin mounting plug that was placed within a port at the top of the vessel near the vessel orifice. The transducer was oriented so that the measuring face was parallel to the flow of the venting refrigerant. This was done to avoid the impact of liquid droplets, generated during the vaporization process, with the transducer face. The output of the pressure transducer was recorded by a LeCroy 9314M digital oscilloscope and transferred to a personal computer for further processing.

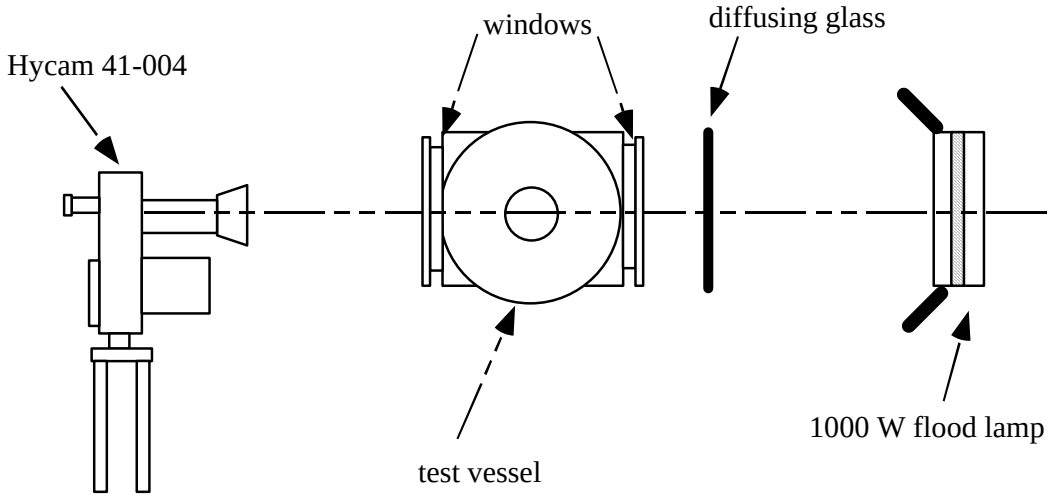


Fig. 2.7 Schematic diagram of high-speed photography setup.

To visualize the boiling phenomenon, a 16-mm Hycam high-speed camera was used, operated at framing rates between 1000 and 5000 frames/s. The camera was triggered manually just before the diaphragm was ruptured. To provide lighting for the experiment a 1000 W flood lamp was placed behind the test vessel with diffusing glass used to provide even illumination (see Fig. 2.7).

## 2.6 Test Fluid

Refrigerant-22 was chosen as the test fluid for the present tests due to its thermodynamic similarities to propane and the fact that it is not flammable. Table 2.1 shows selected thermodynamic properties of refrigerant-22 and propane to illustrate their similarities. Figure 2.8 shows a comparison of the liquid-vapor saturation curves for Refrigerant-22 and propane.

Table 2.1 Comparison of selected thermodynamic properties of Refrigerant-22 and propane

| Property | Unit | Refrigerant 22 | Propane |
|---|---|---|---|
| Chemical Formula | - | $CHClF_2$ | $C_3H_8$ |
| Chemical Name | - | Difluorochloromethane | Propane |
| Molecular Weight | kg/kg-mol | 86.48 | 44.09 |
| Boiling Point @ 1 atm | K | 232.41 | 231.25 |
| Vapor Pressure @ 25ºC | MPa | 1.039 | 0.9478 |
| Critical Temperature | K | 369.17 | 369.82 |
| Critical Pressure | MPa | 4.9776 | 4.2362 |
| Critical Density | $kg/m^3$ | 524.77 | 197.38 |
| Specific Heat Vapor @ 25ºC | J/kg-K | 863 | n/a |
| Specific Heat Liquid @ 25ºC | J/kg-K | 1236 | n/a |
| Latent Heat of Vaporization @ 25ºC | kJ/kg-K | 180.6 | 335.18 |
| Surface Tension @ 25ºC | $N/m \times 10^3$ | 7.95 | n/a |

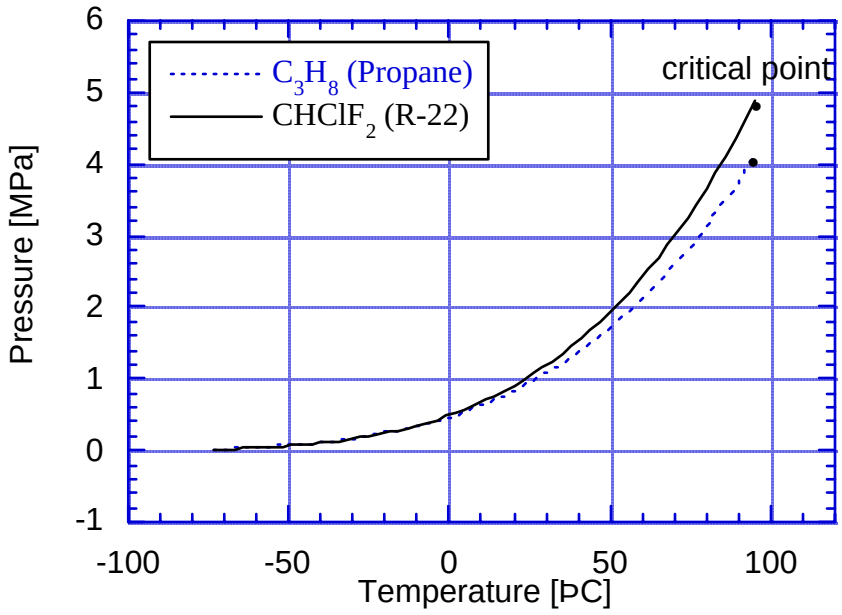


Fig. 2.8 Comparison of liquid-vapor saturation curves for Refrigerant-22 and propane.

# 3. RESULTS AND DISCUSSION

Although test sections with three different geometries were used in the present investigation, the behavior of the pressure history within each of the vessel was similar following depressurization. Prior to examining the specific results for each geometry, the characteristic pressure history will be described to introduce the nomenclature used in subsequent sections.

## 3.1 General Features of Pressure History

Figure 3.1 shows a comparison between the characteristic pressure history recorded within the steel vessel following depressurization of R-22 (90% liquid fill, initial pressure 1.38 MPa, orifice diameter 1.9 cm) with an experiment at the same initial conditions using ambient temperature water pressurized with air. For the experiment with water, following diaphragm rupture little pressure recovery is observed due to the low vapor pressure of water. In contrast, when depressurized, the liquid R-22 boils rapidly causing a transient repressurization of the vessel, followed by a slow pressure decay to atmospheric pressure on a much longer time scale. The initial rates of depressurization differ due to the larger molecular weight of the refrigerant compared to air.

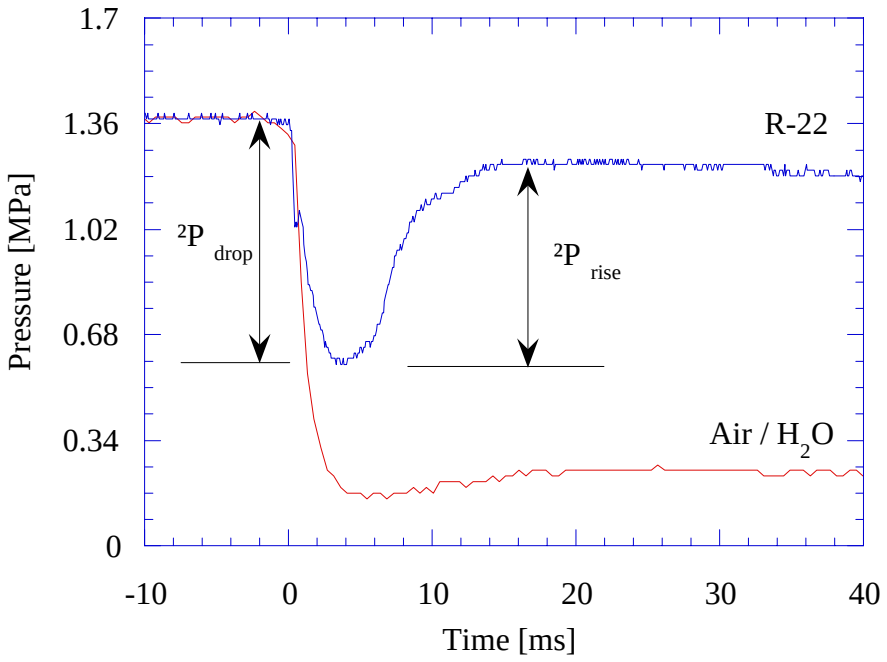


Fig. 3.1 Comparison of characteristic pressure history for venting of R-22 and pressurized water.

Figure 3.1 also shows the definition of the pressure drop $DP_{drop}$ and repressurization $DP_{rise}$, that are reported in later figures.

If the steel test section is placed horizontally with the face of pressure transducer *facing* the free surface of the liquid, the pressure history recorded following depressurization of the liquid is shown in Fig. 3.2. In this case, liquid droplets torn from the liquid surface during the rapid boiling process directly impact the transducer face, producing a series of short pressure spikes with a duration of 0.1–0.2 ms.

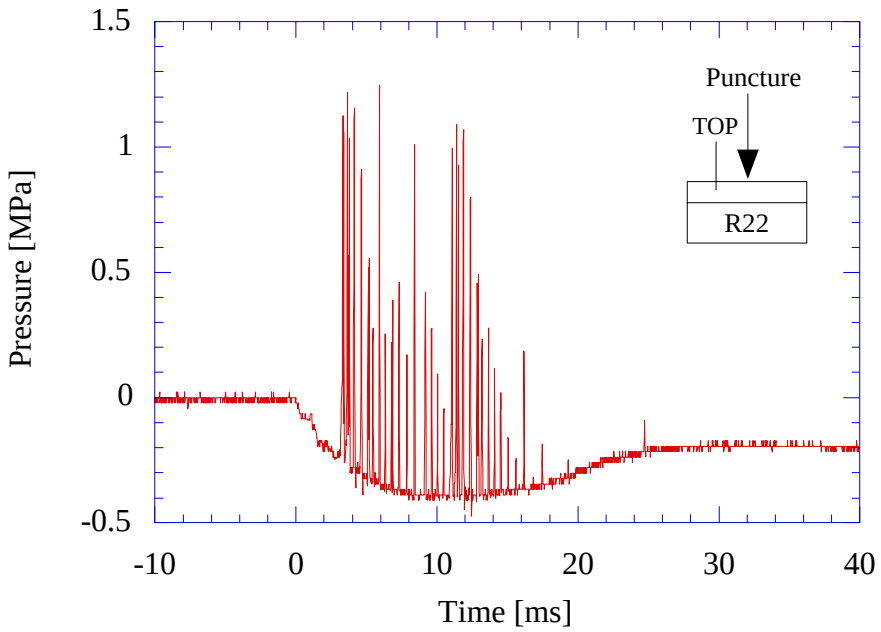


Fig. 3.2 Pressure history recorded for horizontal test section illustrating pressure spikes generated by impact of liquid droplets with pressure transducer face.

Similar results have also been reported by Ogiso et al. (1972) who used a long vertically mounted tube filled with compressed heated water with pressure transducers mounted along the length and at both ends of the tube. Upon sudden depressurization from a vent near the top, the transducers located at the top end measured very large and rapid pressure impulses. These impulses were attributed to the impact of liquid droplets colliding against the pressure transducer sensing element.

In all subsequent tests reported in the present study, the transducer surface was mounted perpendicular to initial liquid free surface to avoid the impact of liquid droplets during the two-phase venting process.

### 3.2 Parametric Investigation with Rectangular Steel Vessel

A parametric study was carried out to examine the influence of vent area, liquid fill volume and initial liquid pressure on the boiling dynamics in the 260 ml steel vessel containing Refrigerant-22.

Figure 3.3 shows the effect of increasing the orifice area on the normalized pressure history within the vessel for 90% liquid fill and for orifice diameters ranging from 0.4 cm to 1.9 cm. Increasing the orifice area increases the rate of venting and hence increases the rate and amount of depressurization, as shown in Fig. 3.4. Figure 3.5 shows the effect of liquid volume fraction on the pressure history for an initial pressure of 3.15 MPa in each case. The rate of pressure drop and rise are both increased as the amount of liquid increases (corresponding to a smaller initial vapor volume). Figure 3.6 shows that as the liquid fill volume increases, the nondimensional pressure drop increases, but the nondimensional pressure rise stays approximately constant. The relationship between the amount of initial pressure drop within the vessel and the subsequent amount of pressure rise is shown in Fig. 3.7 for two different fill volumes in the steel vessel. The data indicate that there exists a strong correlation between the degree of superheat attained by the liquid (which is proportional to the amount of depressurization) and the corresponding amount of repressurization for a given liquid fill volume and rupture area.

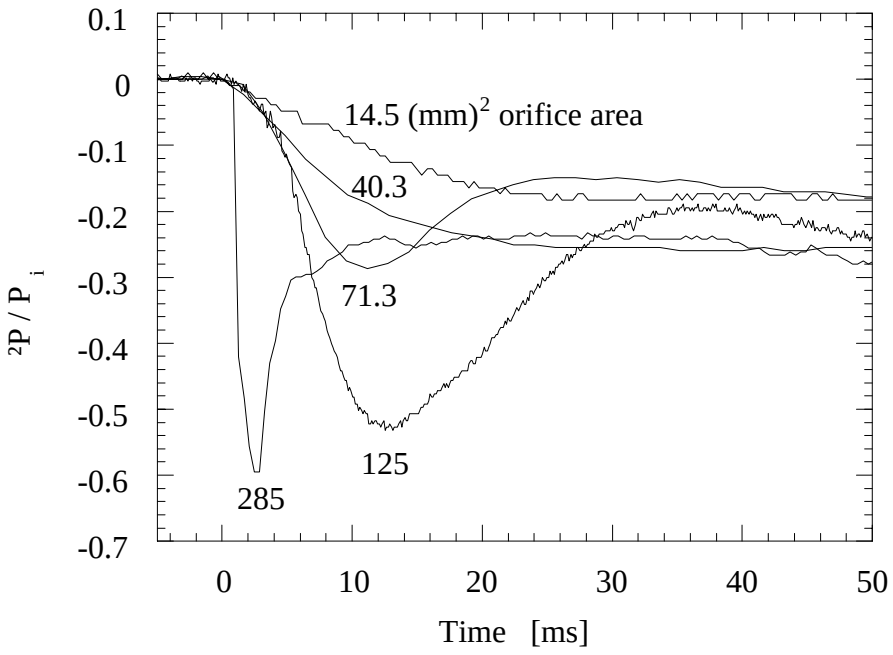


Fig. 3.3 Effect of orifice area on pressure history for 90% liquid fill.

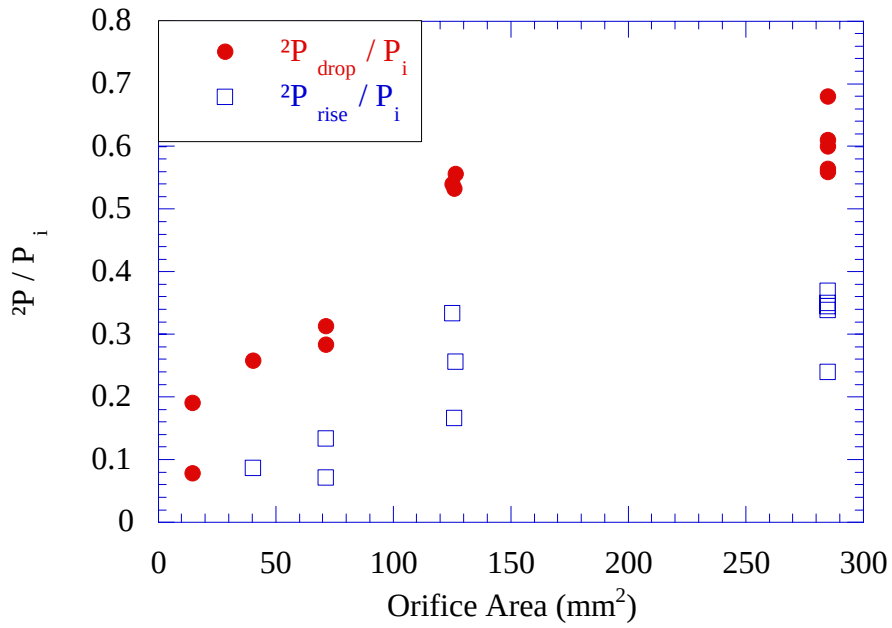


Fig. 3.4 Effect of orifice area on degree of depressurization and repressurization.

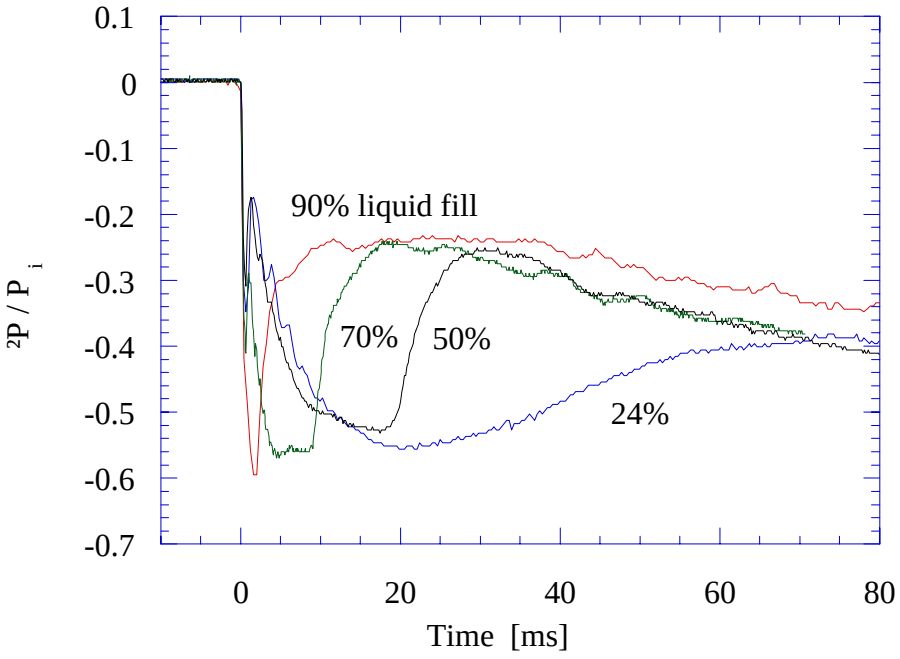


Fig. 3.5 Effect of initial liquid volume on pressure history. Initial pressure is 3.15 MPa.

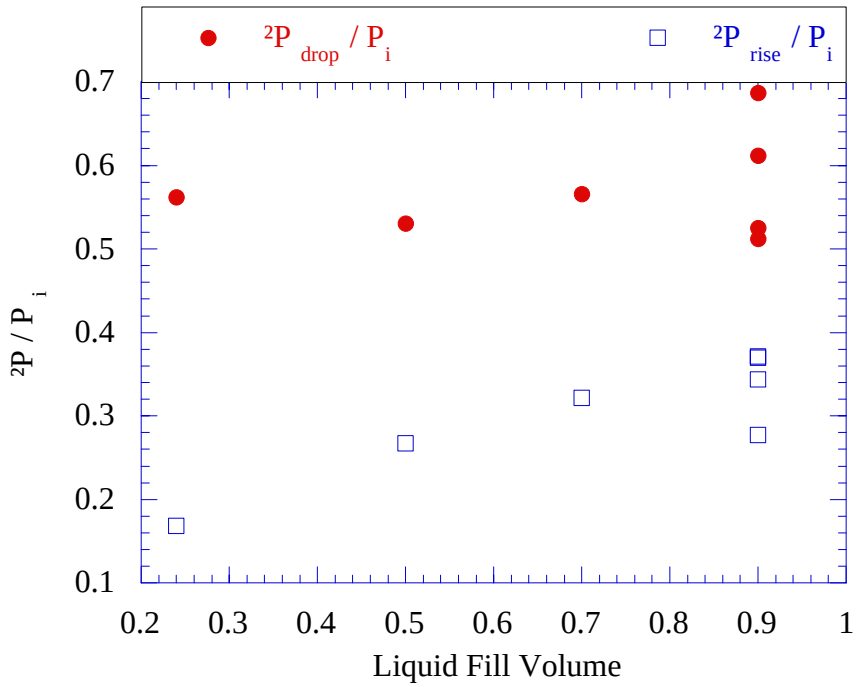


Fig. 3.6 Effect of liquid fill volume on the degree of depressurization and repressurization.

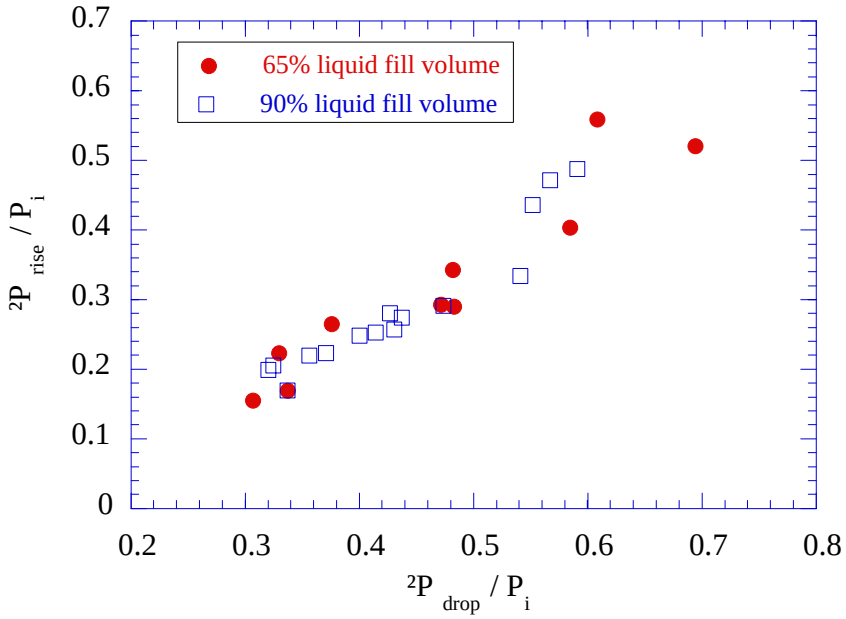


Fig. 3.7 Relationship between pressure rise and pressure drop for trials with steel vessel.

Of particular interest is how the violence of the boiling response, as characterized by the amount of pressure recovery within the vessel, depends on the initial thermodynamic state of the liquid. Figure 3.8 shows how the pressure rise varies with the initial saturated liquid pressure for a constant orifice area of 1.9 cm and liquid fill volumes of 65% and 90%. The degree of repressurization reaches a maximum at about 2 MPa for liquid fill volumes of both 65% and 90%. The initial pressure for which the maximum occurs is close to the initial pressure at which the greatest superheat can be attained following depressurization of the saturated liquid to atmospheric pressure.

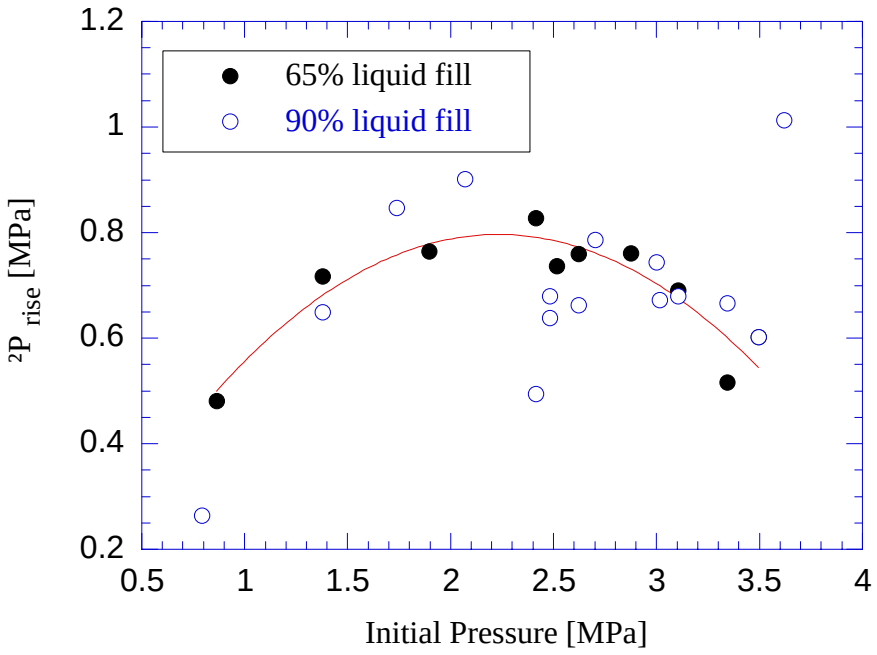


Fig. 3.8 Degree of repressurization as a function of initial pressure within steel vessel. The curve represents a second order polynomial fit through the 65% fill data.

Figure 3.9 shows the saturation and spinodal curves for R-22 which bound the metastable region. Path 1-2 corresponds to an isentropic expansion from a pressure of 2.06 MPa (and a saturation temperature of 53˚C) to atmospheric pressure which yields the greatest possible degree of superheat at atmospheric pressure. The state of the liquid following depressurization for both the 65% and 90% liquid fill volume trials is also shown in Fig. 3.9. Although no homogeneous boiling was observed, the locus of data points indicates that there is a limit of superheat attained that is determined by heterogeneous boiling. Even though the degree of superheat attained will depend on the geometry of the vessel as well as the surface properties of the vessel walls, it is interesting to note that the maximum degree of superheat is attained at a liquid temperature that is similar to that predicted by homogeneous nucleation theory.

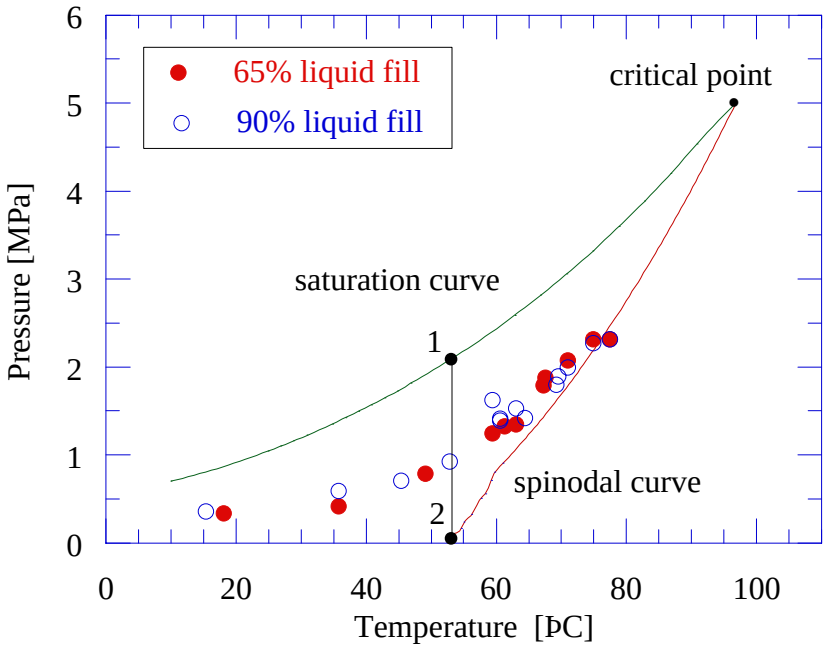


Fig. 3.9 Locus of thermodynamic end states following pressure drop showing the degree of superheat attained for the steel test vessel.

### 3.2.1 Visualization of Boiling in Rectangular Steel Vessel

The characteristics of the boiling process inside the 260 ml steel vessel were observed with high-speed photography. Figure 3.10 shows a series of high-speed photographs illustrating the boiling process during the initial depressurization process, with an orifice diameter of 1.9 cm and an initial pressure of 1.03 MPa. Heterogeneous nucleation on the walls dominates and the boiling propagates from the side walls towards the center of the vessel as a wavefront with an average speed of the order of 1 m/s. Since the liquid never reaches the superheat limit, homogeneous nucleation within the bulk of the liquid does not occur.

Figure 3.11 shows a series of photographs with a close-up view of the test section during the depressurization of the Refrigerant-22 from an initial pressure of 1.43 MPa and the same orifice area as for Fig. 3.10. Also shown in the figure is the corresponding pressure history within the vessel with the times of the photographs noted on the graph. Note that when the pressure reaches a minimum value within the vessel, vapor generated on both sides of the vessel has nearly penetrated across to the centre of the test section. Also note the growth of several pre-existing bubbles within the liquid on the right side of the photographs.

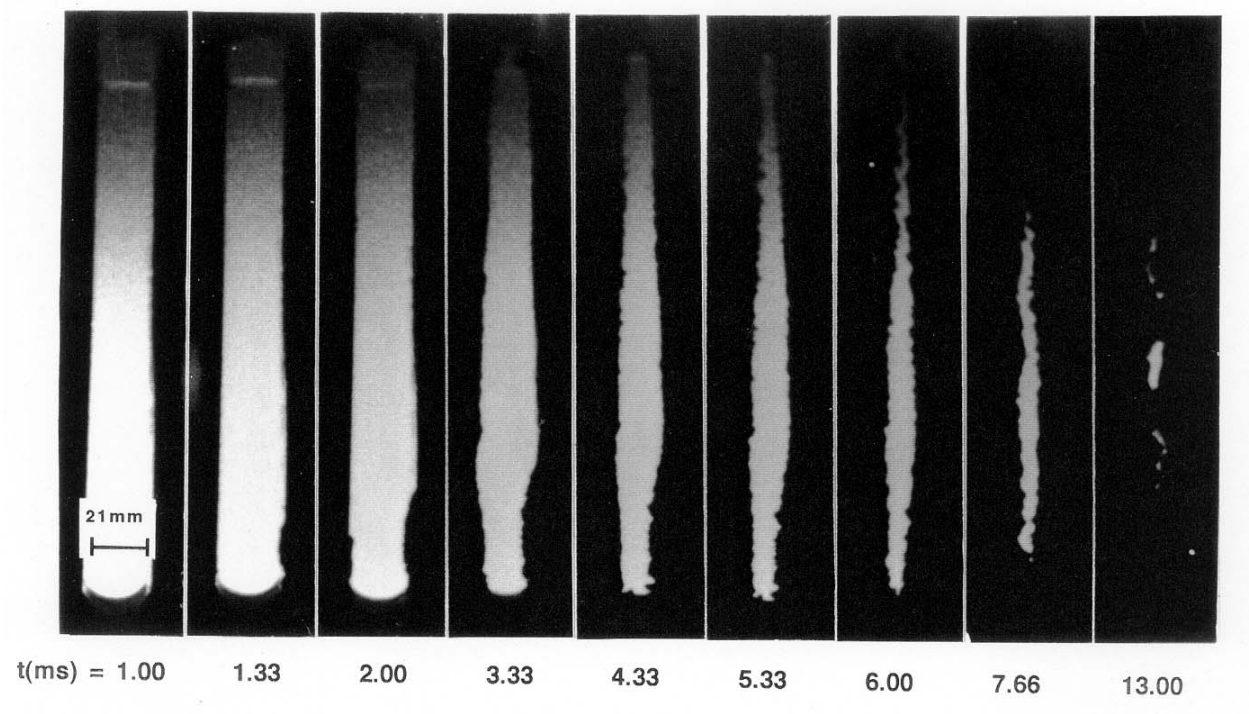


Fig. 3.10 Sequence of high-speed photographs showing heterogeneous boiling of R-22 from the walls in the 260 ml steel vessel ($P_i$ = 1.03 MPa).

## 3.3 Parametric Investigation with Cylindrical Glass Vessel

The next series of trials was performed in the 75 ml glass tube (25 mm inner diameter) using a 9.5 mm diameter orifice and 90% fill volume. Figure 3.12 shows that the normalized pressure rise increased with normalized pressure drop, showing a similar behavior as that observed in the steel tank. However, for a given initial pressure, larger pressure drops were observed in the glass vessel, due to a reduction in the number of nucleation sites on the glass surface as compared to the wall of the steel vessel. Figure 3.13 shows the variation of the pressure drop and corresponding pressure rise as a function of the initial pressure. Once again, the pressure rise appears to reach a maximum value for an initial pressure of about 2 MPa, similar to the results for the steel vessel (see Fig. 3.8).

### 3.3.1 Visualization of Boiling in Cylindrical Glass Vessel

With the cylindrical glass vessel, two modes of boiling were observed which depended on the initial temperature of the liquid. For initial R-22 temperatures less than 25˚C (corresponding to saturation vapor pressures less than 1.03 MPa) the boiling occurred as an evaporation wave moving from the free surface of the liquid vertically downwards. Figure 3.14 shows an enlarged view of the liquid-vapor interface in the early stages following depressurization. After the diaphragm is ruptured, the vapor above the liquid condenses, signaling the passage of an

expansion wave, and 7.33 ms later the surface of the liquid erupts violently into a two-phase flow consisting of vapor and fine droplets moving vertically at high speed. A detailed discussion of the mechanism of propagation of the evaporation wave can be found in Hill (1991).

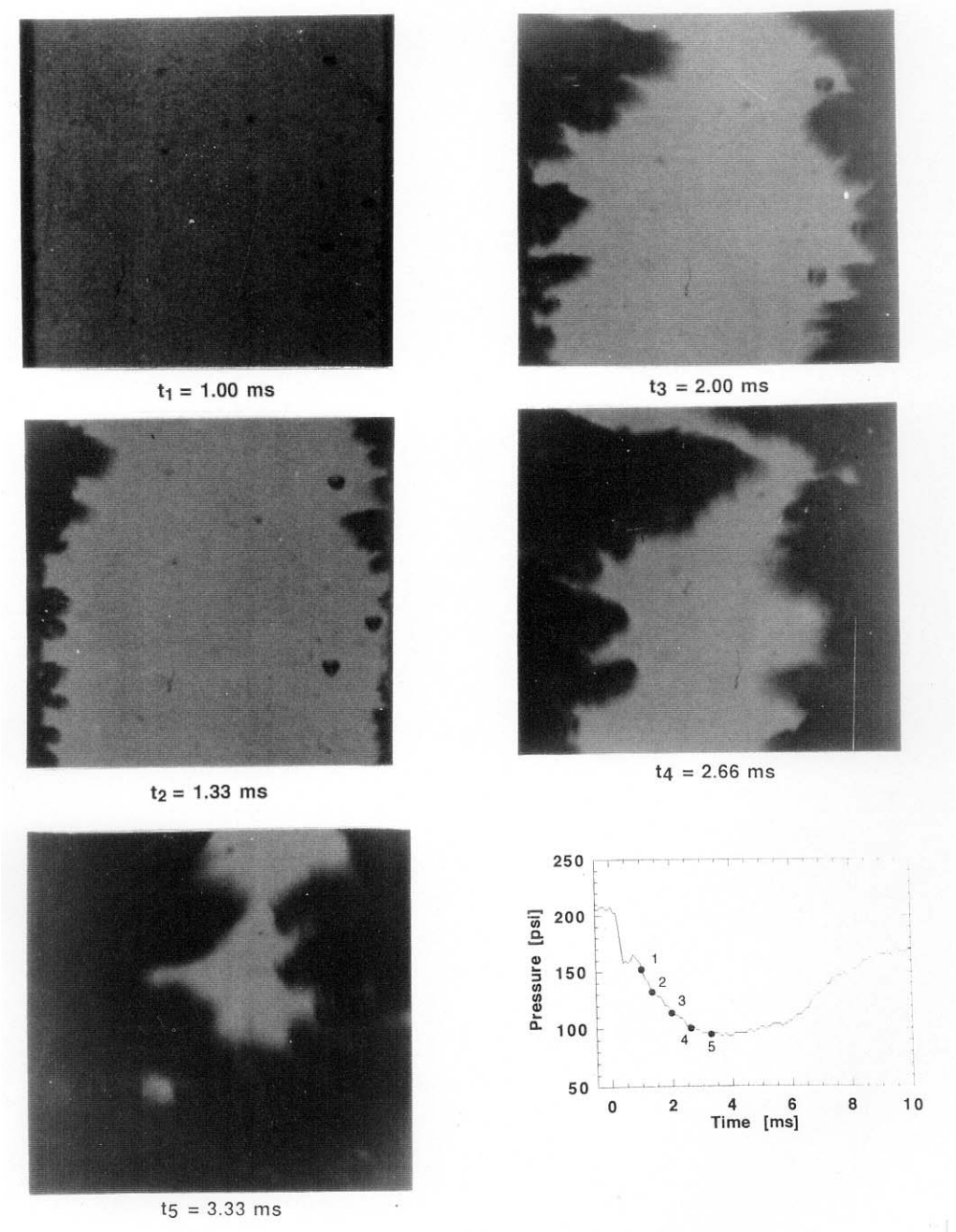


Fig. 3.11 Sequence of high-speed photographs showing heterogeneous boiling of R-22 from the walls of steel vessel with an initial pressure of 1.43 MPa.

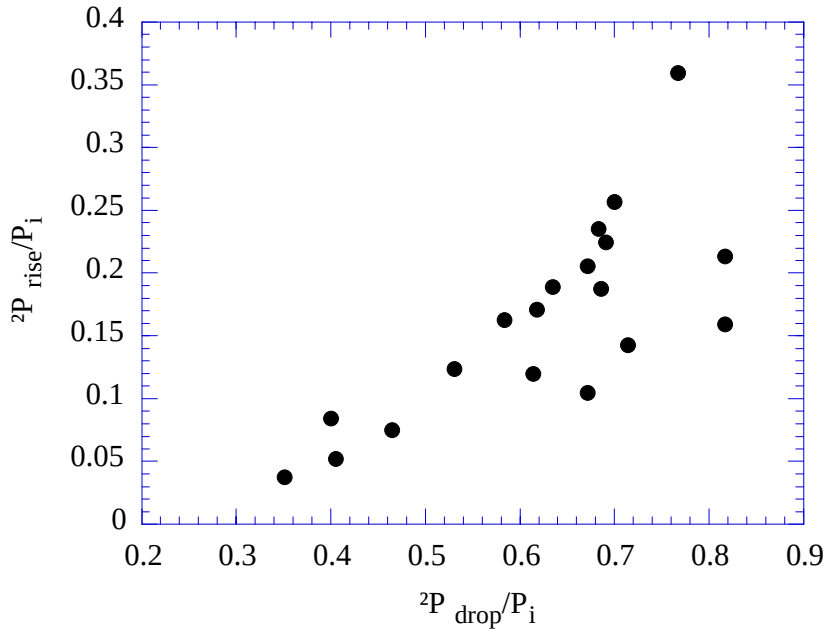


Fig. 3.12 Normalized pressure rise as a function of normalized pressure drop for the 75 ml cylindrical glass vessel.

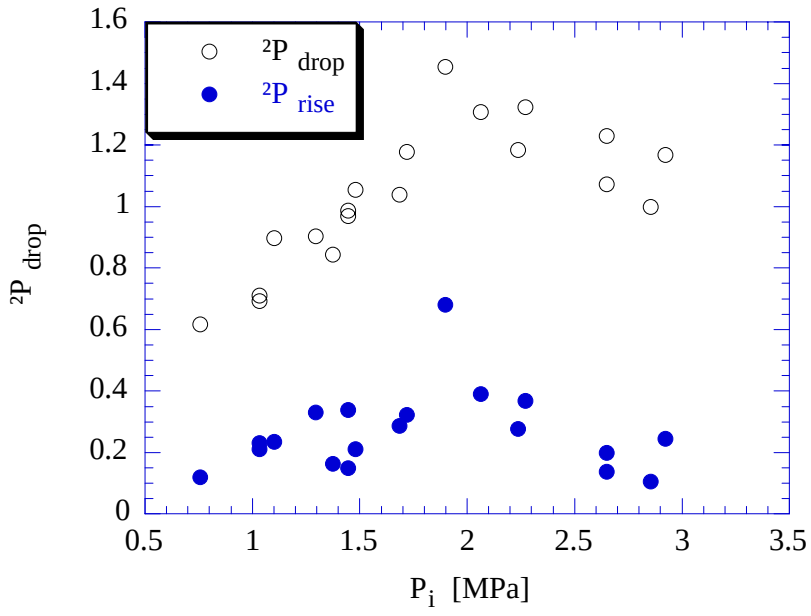


Fig. 3.13 Pressure drop and rise as a function of the initial pressure in the 75 ml cylindrical glass vessel.

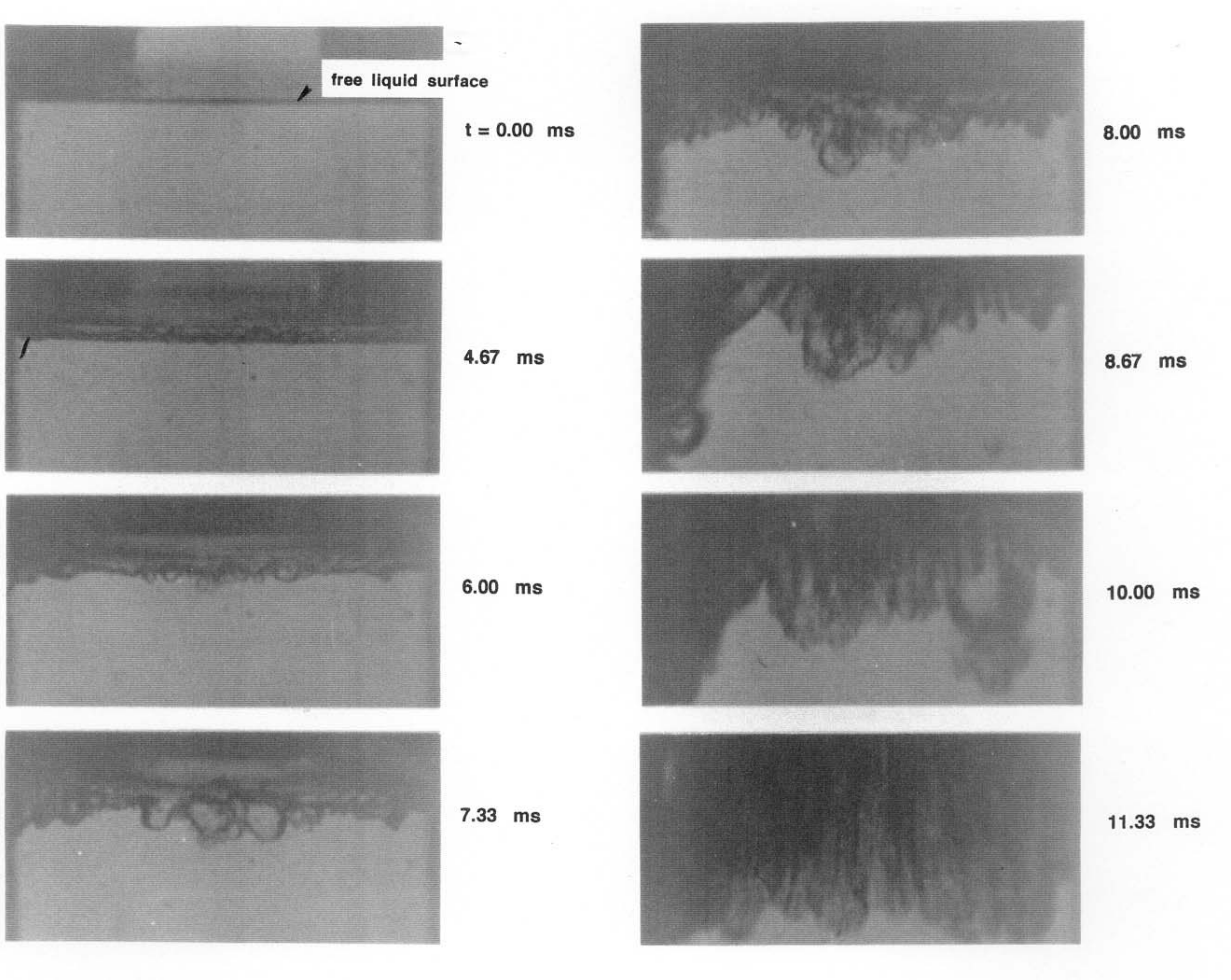


Fig. 3.14 Breakup of free surface of liquid R-22 contained within a glass tube following depressurization ($P_i$ = 1.20 MPa).

The propagation of the evaporation wave into the superheated liquid is illustrated in Fig. 3.15 which shows a sequence of photographs for an initial pressure of 1.03 MPa. The initial burst of nucleation at the liquid surface preferentially starts on one side and the evaporating front remains somewhat asymmetric during its propagation. Contours of the evaporation wavefront were taken from the high-speed photographs and are shown in Fig. 3.16 with the corresponding displacement and velocity of the front shown as a function of time in Fig. 3.17. During the initial startup phase, the front velocity is quite large and erratic; however, after several hundred milliseconds, the front velocity levels off at a value of about 0.1 m/s.

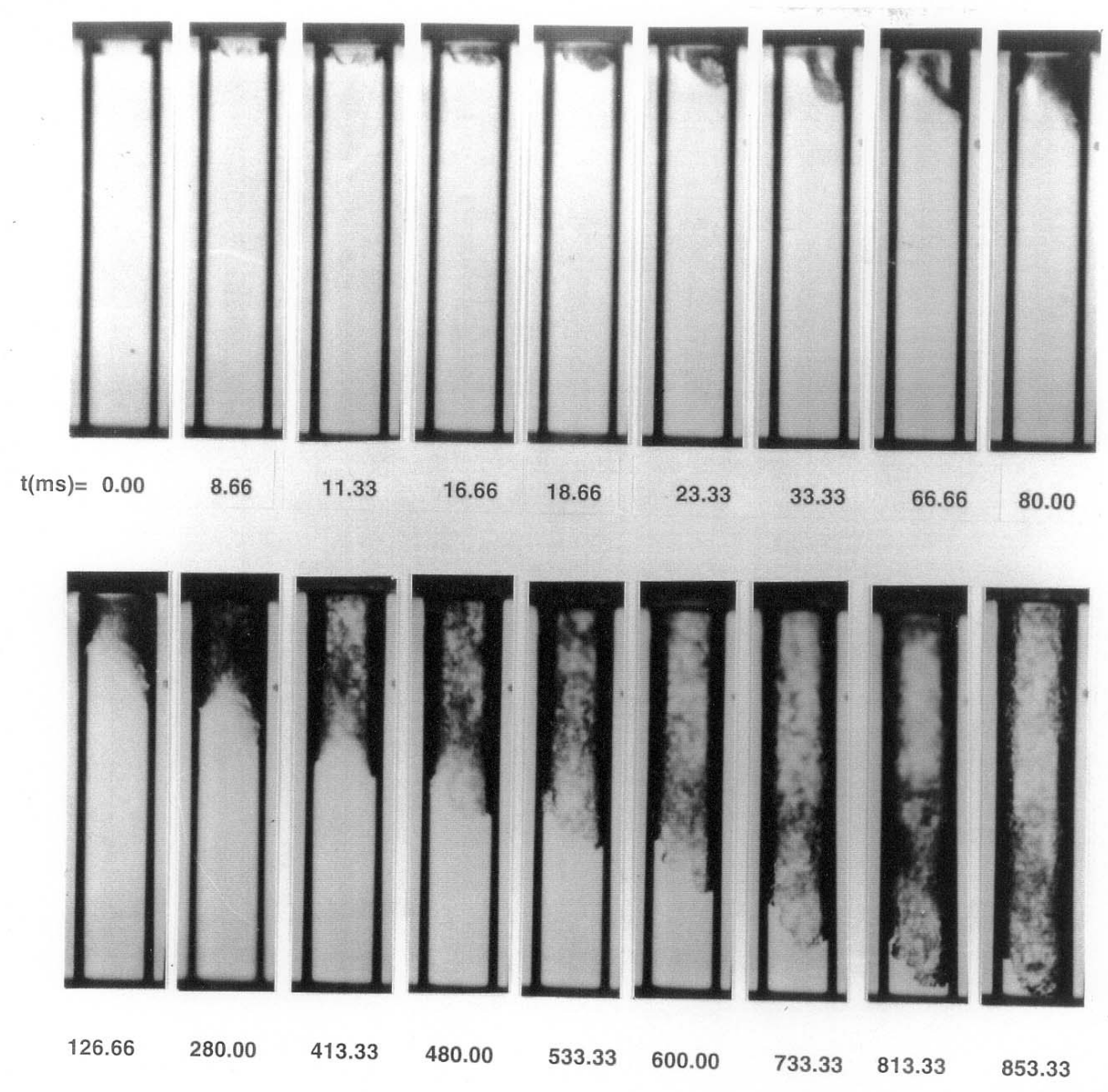


Fig. 3.15 Sequence of high-speed photographs showing the propagation of an evaporation wave into superheated R-22 in a glass tube ($P_i$ = 1.03 MPa).

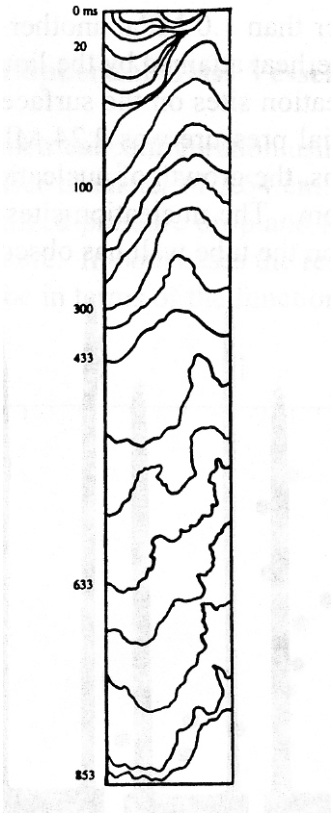


Fig. 3.16 Contours (shown as a mirror image) of the boiling front shown in Fig. 3.15.

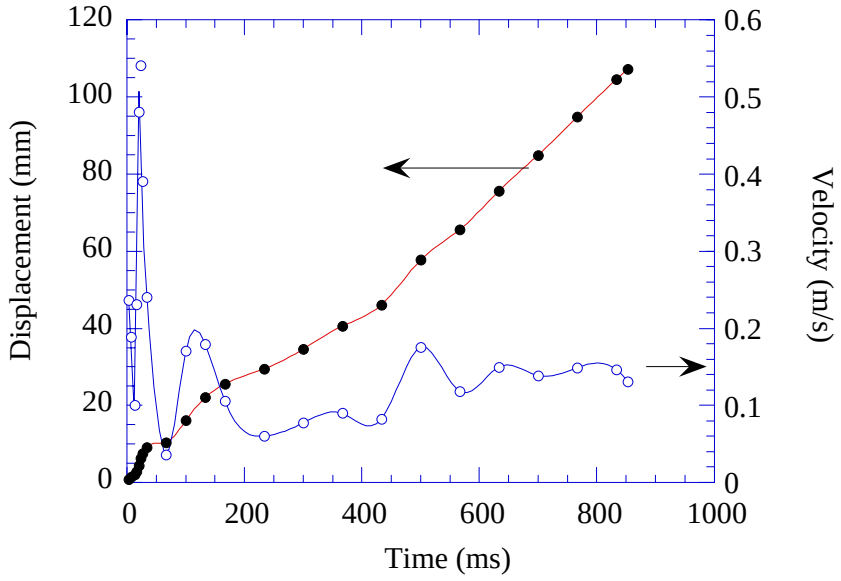


Fig. 3.17 Variation of displacement and velocity of boiling wavefront estimated from Fig. 3.16.

For initial pressures greater than 1.0 MPa, another mode of nucleation occurs within the glass vessel. In this case the superheat attained by the liquid following depressurization is sufficient to induce the growth of nucleation sites on the surface of the glass. This situation is illustrated in Fig. 3.18 in which the initial pressure was 2.24 MPa. At a time of t = 0 ms, the diaphragm is ruptured. After about 11 ms, the growth of nucleation sites is first visible about half way down the tube and near the bottom. The nucleation sites grow and coalesce and by about 40 ms the growth of nucleation sites on the tube wall has obscured the two-phase mixture within the tube.

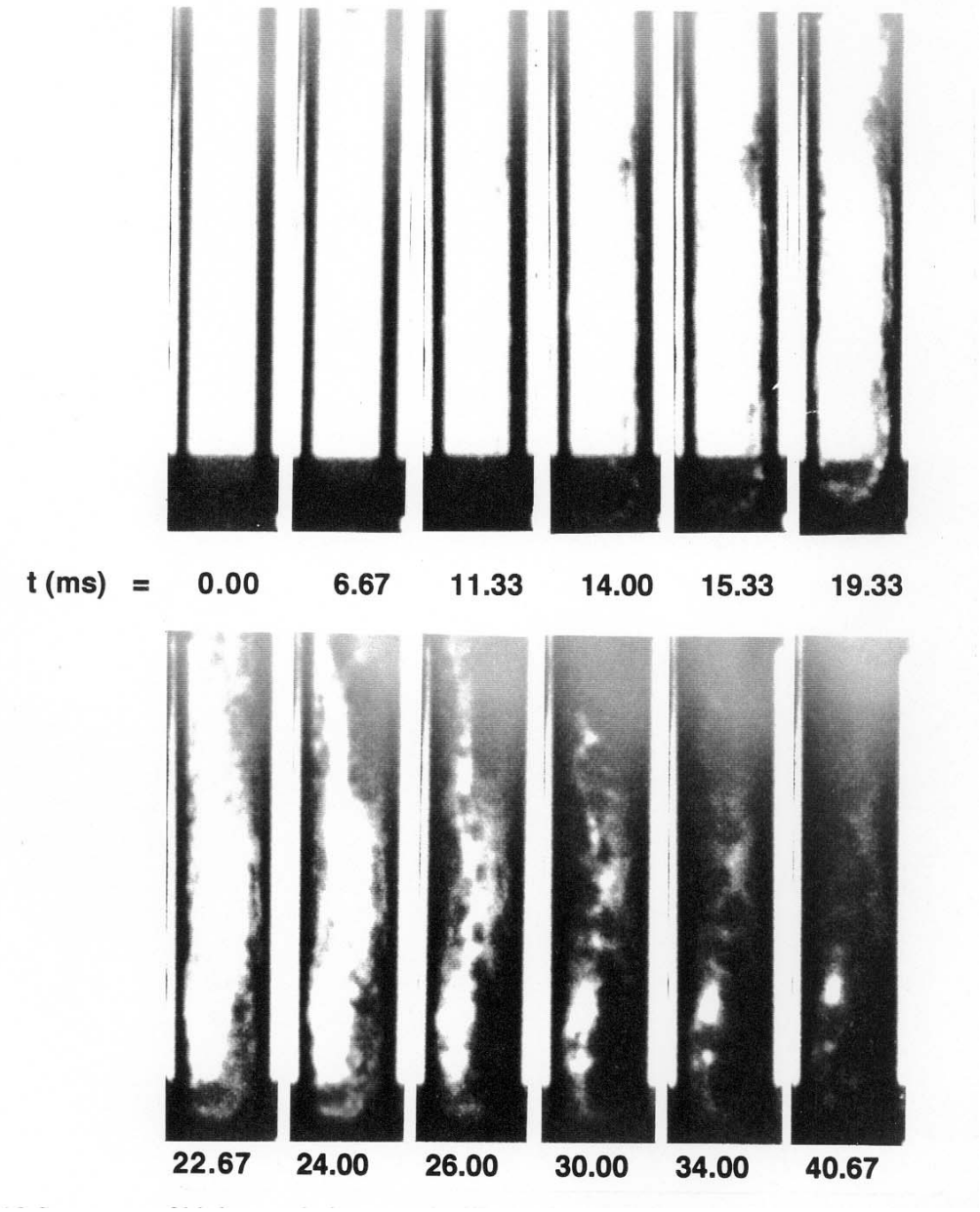


Fig. 3.18 Sequence of high-speed photographs illustrating the heterogeneous nucleation on the wall of the glass tube for an initial pressure of 2.24 MPa.

### 3.4 Parametric Investigation with Spherical Glass Vessel

Tests were carried out in a third geometrical configuration using 150 ml spherical glass flasks with a 90% liquid fill volume and an orifice diameter of 2.54 cm. Figure 3.19 shows the normalized pressure rise as a function of normalized pressure drop and Fig. 3.20 shows the repressurization recorded as a function of initial pressure. In both cases the results are similar to the earlier results with the steel vessel and the glass tube in terms of the functional dependence.

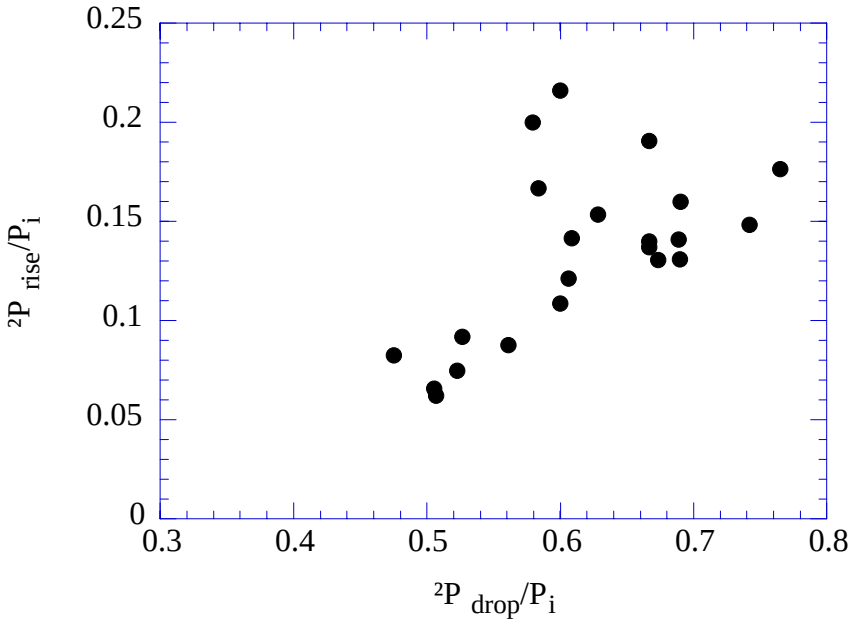


Fig. 3.19 Normalized pressure rise as a function of normalized pressure drop for 150 ml spherical glass vessel with 90% liquid fill volume and an orifice diameter of 2.54 cm.

To determine the effect of the presence of nucleation sites within the bulk of the liquid, the tests were repeated with the addition of a ball (about 3 cm long and 2 cm wide) of steel wool placed inside the liquid within the sphere. The addition of the steel wool resulted in a decrease in the amount of depressurization and an increase in the time for the pressure to fall to a minimum and the subsequent time to rise to a maximum pressure (both times were increased by a factor of about 5). However, more significantly, although the pressure drop (and hence the superheat attained by the liquid) decreased, the subsequent pressure rise increased. This effect is illustrated in Fig. 21 which shows the data from Fig. 20 repeated with the addition of the results with the addition of the steel wool.

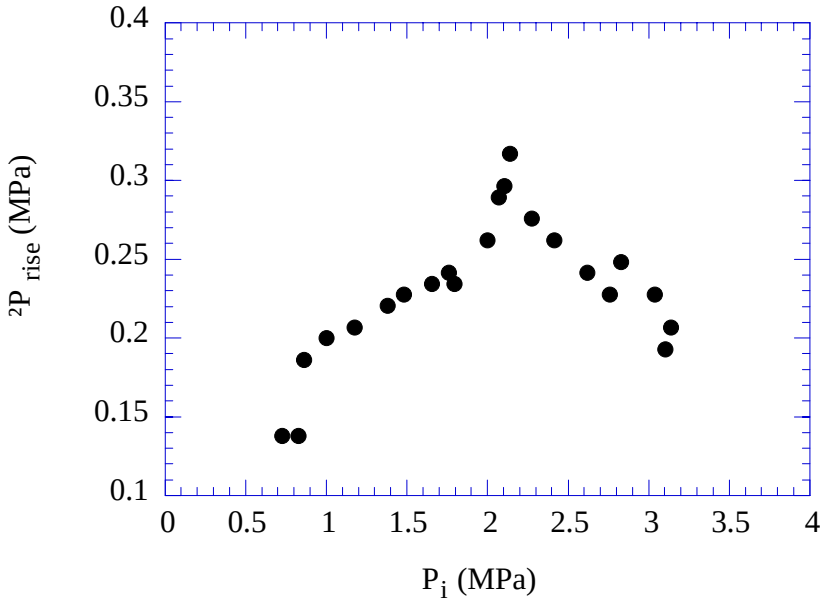


Fig. 3.20 Repressurization as a function of initial vessel pressure for the spherical glass vessel with 90% liquid fill volume.

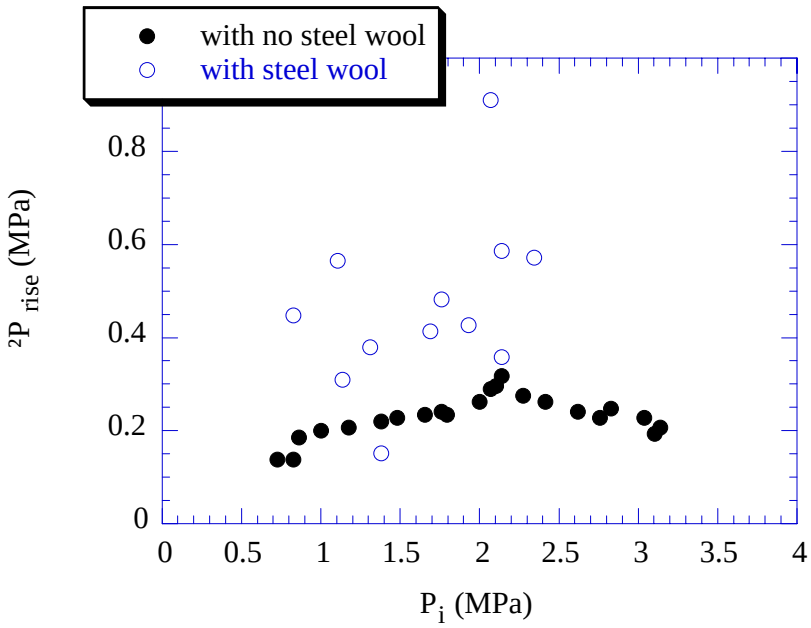


Fig. 3.21 Comparison of the repressurization as a function of initial vessel pressure with and without the presence of a ball of steel wool within the bulk of liquid.

### 3.4.1 Visualization of Boiling in Spherical Glass Vessel

For initial pressures below 1 MPa, the boiling of the liquid proceeds once again by means of an evaporation wave, similar to that observed in the cylindrical glass vessel. This is illustrated in Fig. 3.22 which shows high-speed photographs taken from an experiment using a *50* ml glass sphere with an initial pressure of 1.0 MPa.

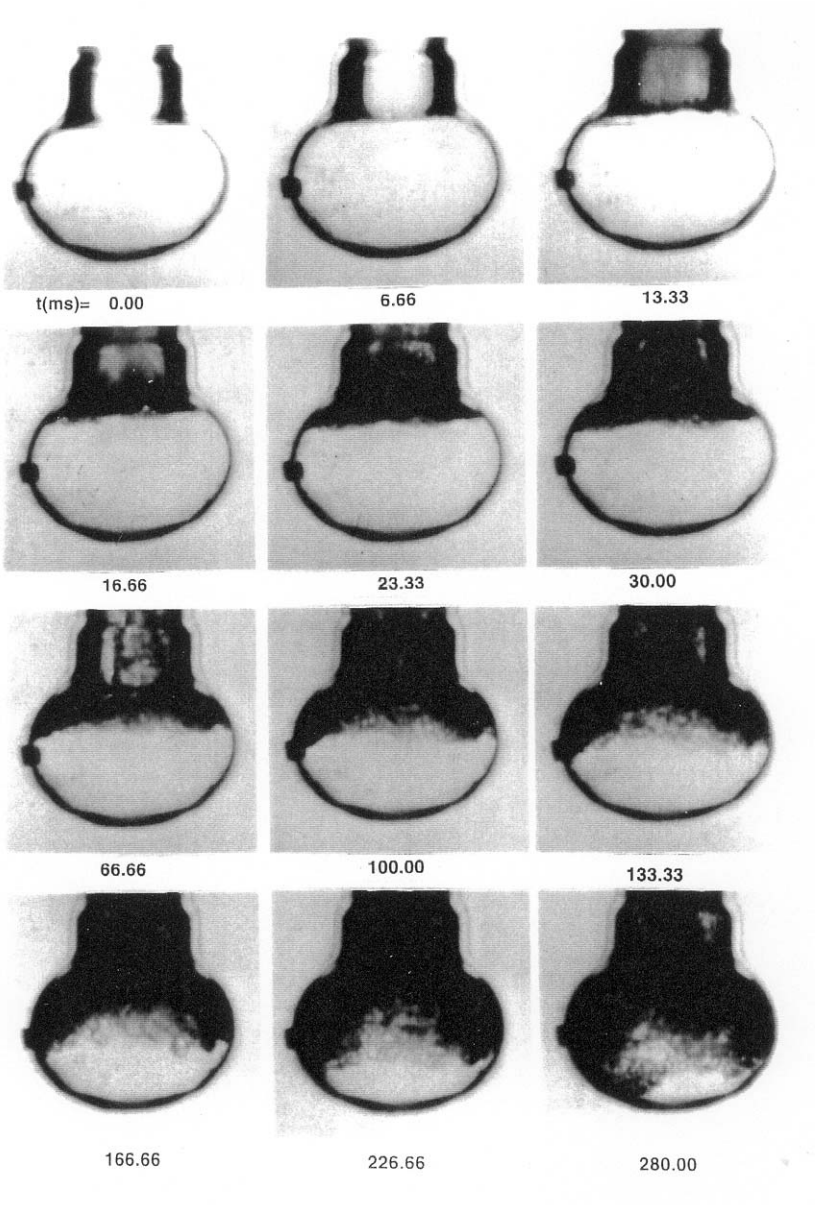


Fig. 3.22 Sequence of high-speed photographs showing the propagation of an evaporation wave within a 50 ml glass sphere. The initial liquid free surface is located at the junction between the sphere and the neck.

# 4. CONCLUSIONS AND RECOMMENDATIONS

The explosive boiling response of suddenly depressurized Refrigerant-22 was investigated experimentally in three different small-scale vessels: (i) a 260 ml steel vessel with a rectangular test section, (ii) a 75 ml cylindrical glass tube and (iii) a 150 ml glass sphere. In all cases, rapid boiling caused a repressurization within the vessels which was approximately linearly dependent on the pressure undershoot or the degree of superheat attained by the liquid. The degree of repressurization reached a maximum value in all three vessels at an initial pressure of about 2 MPa, regardless of the mode of boiling, vessel geometry or liquid fill volume. The mode of nucleation observed depended primarily on the degree of superheat attained by the liquid as well as the surface characteristics of the vessel. For the steel vessel, heterogeneous boiling from the walls dominated. In the glass tube a self-sustained evaporation wave propagated from the free surface into the liquid for initial pressures at and below 1 MPa. For an initial pressure of 1 MPa, after an initial startup phase lasting about 200 ms, the evaporation wave attained an average velocity between 5 and 20 cm/s. Since the wave velocity is relatively slow, fluctuations of the pressure in the vessel downstream of the wave due to the competition between the rates of vaporization and venting can influence the propagation of the wave. Deviations of the wavefront from a planar shape corresponded to an increase in the average propagation velocity and may be caused by spatial variations in the liquid temperature. For large initial pressures, the boiling in the present experiments was dominated by wall boiling so that the ratio of surface area/liquid volume played an important role in the rate of vapor generation. Therefore the present results cannot easily be scaled in a quantitative manner to larger scale cylindrical or spherical vessels, where boiling on the walls will be relatively less important compared to boiling within the bulk of the liquid. Nevertheless, the trends observed in the present tests, in particular that the violence of the boiling increases with initial pressure or temperature up to a maximum corresponding approximately to the superheat limit temperature at atmospheric pressure (~ 53ºC), are expected to be reproduced in larger scale tests. In additional tests, the number of nucleation sites present within the liquid prior to depressurization was increased substantially by placing a ball of steel wool into the liquid. This had the effect of lowering the "activation energy" for boiling to begin which reduced the amount of depressurization that was attained and increased the characteristic time for the pressure fall and rise. However, the growth of the large number of nucleation sites present in the liquid bulk due to the steel wool actually augmented the degree of repressurization within the test section.

Regardless of the initial conditions, the most violent boiling will occur if the liquid is brought uniformly to its limit of superheat. Therefore, from a practical point of view regarding the storage of liquefied gases, situations that lead to large rates and degrees of depressurization, such as large vent areas and liquid fill volumes, should be avoided. The initial vessel pressure should be maintained, if possible, at a level such that the superheat limit cannot be attained, even for rapid venting of the liquid to atmospheric pressure. For propane, this corresponds to a pressure of about 1.8 MPa, associated with a saturation pressure of 53˚C. In any case, the pressure relief valve should be set at a level as low as possible, given the ambient temperature conditions. This will minimize the thermal energy stored in the liquid and vapor within the vessel. Minimizing the stored energy will minimize the potential work associated with the expansion of the vessel contents to atmospheric pressure following loss of containment, as well as the potential associated blast and projectile hazards.

## REFERENCES


Alamgir, M. and Lienhard, J. H. "Correlation of Pressure Undershoot during Hot Water Depressurization," J. *Heat Transfer*, Vol. 103, 1981, pp. 52-55.

Avedisian, C.T., "Bubble growth in superheated liquid droplets," in Encyclopedia of Fluid Mechanics, Gulf Publishing Co., Houston, Texas, 1986, pp. 130-190.

Barbone, R., "Explosive Boiling of a Depressurized Volatile Liquid," M.Eng. Thesis, Department of Mechanical Engineering, McGill University, 1994.

Bartak, J., "A Study of the Rapid Depressurization of Hot Water and the Dynamics of Vapour Bubble Generation in Superheated Water," *Int. J. of Multiphase Flow* , Vol. 16, No. 5., 1990, pp. 789-798.

Birk, A.M., Ye, Z., Maillette, J. and Cunningham, M., "Summary on medium scale fire tests investigating the BLEVE event," *Internal Report for TDC Transport Canada*, 1991.

Birk, A.M., and Cunningham, M. H., "The boiling liquid expanding vapour explosion," *J. Loss Prev. Process Ind.*, Vol. 7, No. 6, 1994, pp. 474-480.

Chaves, H., Lang, H., Meier, G.E.A. & Speckmann, H.-D., *Lecture Notes in Physics: Flow of Real Fluids*, edited by G.E.A. Meier and F. Obermeier, Spinger Berlin, 1985.

Friedel, L. and Purps, S., "Models and Design Methods for Sudden Depressurization of Gas/Vapor-Liquid Reaction Systems," *Int. Chem. Eng.*, Vol. 26, No. 3, 1986, pp. 396-407.

Hanaoka, Y., Maeno, K., Zhao, L., and Heymann, G., "A study of liquid flashing phenomenon under rapid depressurization*," JSME Int. Journal*, Series II, Vol. 33, No. 2, 1990, pp. 276-282.

Hervieu, E., "Behavior of a Flashing Liquid within a Vessel following Loss of Containment: Application to Propane," *ANS Proc. 1992 National Heat Transfer Conference*, Vol. 6, pp. 227-235.

Hill, L.G. and Sturtevant, B., "An experimental study of evaporation waves in a superheated liquid," IUTAM Symposium, Göttingen, Germany, in *Adiabatic Waves in Liquid-Vapor Systems*, edited by G.E.A. Meier and P.A. Thompson, Springer Berlin, 1989, pp. 25-37.

Hill, L. G. "An Experimental Study of Evaporation Waves in a Superheated Liquid," Ph.D. Thesis, California Institute of Technology, 1991.

Ogiso et al., "On the mechanisms of vapor explosions," *Proc. 1st Pacific Chem. Eng. Conf.*, Part II, 1972.

Reid, R.C., “Possible mechanism for pressurized-liquid tank explosions or BLEVE's,” *Science*, Vol. 203, No. 23., 1979, pp. 1263-1265.

Skripov, V.P., *Superheated Liquids*, John Wiley, New York, 1974.

Wormuth, D.W. (ed.), “BLEVE! The Tragedy of San Juanico,” *J. Skandia International*, 1985, pp.1-22.